Complement modulation properties of *Klebsiella Pneumoniae*

Mikkel Eggert Thomsen
Master's Thesis
Medicine with Industrial Specialization
Biomedicine
Aalborg University
2019

Preface

This thesis was done at the Department of Health, Science and Technology at Aalborg University. The work was conducted from the 3rd of September 2018 to the 31th of May 2019, at the Laboratory of Medical Mass Spectrometry under supervision of Assistant Professor, PhD Tue Bjerg Bennike.

I would like to thank Tue Bjerg Bennike for the time and effort invested in keeping the MS-system running, as well as creating a learning environment which has been highly rewarding.

A thank to co-supervisor Professor, DMSc, PhD Svend Birkelund and PhD Fellow Mads Lausen Nielsen for all the inputs throughout this work.

A special thanks to Professor, DMSc Gunna Christiansen for the time spent in providing the electron microscopy micrographs for this work.

Abstract

Klebsiella Pneumoniae is a pathogen of great concern. With the emergence of multi drug resistant strains that cause serious bloodstream infections, the mortality rates for these infections are increasing. Novel therapeutics are hence in urgent need. From a better understanding of the host defense mechanisms against *K. pneumoniae*, new advances in the development of novel therapies can arise. This study investigated how K. *pneumoniae* circumvents the first line of defense, the complement system. By state-of-the-art tandem mass spectrometry (MS) and a novel approach to track the proteolytic cascade of the complement system by N-terminal acetylation, as well as immunoelectron microscopy (IEM), two clinical isolates of *K. pneumoniae* (one serum resistant (391) and one serum sensitive (688)) were analyzed, to test the involvement of human complement regulators in resistance to serum. Results showed that C3 was equally deposited on the two isolates, but for 391 solely in the capsule, where it was rapidly inactivated to iC3b, in a Factor H independent manner. Despite the rapid inactivation, the complement cascade still managed to collect all components of the membrane attack complex (MAC) on isolate 391, as identified by MS, though in significantly lower abundance than on isolate 688. The abundance of clusterin was highest on isolate 391 determined by MS, but IEM showed only clusterin in the outer periphery of the capsule, hence clusterins inhibitory mechanism towards insertion of the membrane attack complex (MAC) in the outer membrane, could not account for the serum resistance of isolate 391. IEM further showed, that the capsule was shedded partly or completely of isolate 391, exposing a surface beneath that did not bind complement components.

Calprotectin, a metal sequester with antimicrobial properties, was identified in high abundance on isolate 391. Calprotectin in association to *K. pneumoniae* is a novel finding, and thus its function unclear. In Helicobacter pylori calprotectin has been shown to induce Lipid A modifications, change in surface charge and biofilm formation. Evidences of a difference in surface charge between the two isolates were further compiled by the findings of components of the coagulation system on isolate 688, that is known to bind negatively charged phospholipids. These findings included plasminogen, Factor V and properdin. Evidence of a novel bacterial C3 convertase was observed on isolate 688, involving properdin, hydrolyzed C3 (C3(H2O)) and Factor B, which also could suggest that the complement resistance can be explained by a change in surface charge.

The study confirmed that N-terminal acetylation of peptides probes proteomics to track the proteolytic cascade of the complement system, which is a gamechanger in complement research. However, results did not manage to identify a mechanism of utilization of human complement regulatory proteins, that could account for the serum resistance seen in isolate 391, however the results showed evidence of a difference in surface charge, which both could explain the morphological changes of the capsule as well as the serum resistance. Yet, further studies have to be done, to confirm this hypothesis, calprotectins role in serum resistance of *K. Pneumoniae*, aswell as the importance of convertases involving C3(H2O).

Dansk resume

Klebsiella pneumoniae er et patogen som kræver stor opmærksomhed. Udviklingen og spredningen af multiresistente stammer, som forårsager kritiske kredsløbs infektioner, har ført til at dødeligheden for disse infektioner er stigende. Der er derfor et kritisk behov for nye behandlingsmuligheder. Ved at opnå en dybere forståelse af det humane immunrespons mod *K. Pneumoniae*, nye skridt i udviklingen mod nye behandlingsmuligheder kan tages. Dette studie tager udgangspunkt i *K. Pneumoniaes* egenskaber til at overleve angreb fra complement system. Ved brug af state-of-the-art tandem masse spektrometri, en innovativ måde at følge den proteolytiske kaskade ved N-terminal acetylering såvel som immunoelektron mikroskopi (IEM), to kliniske *K. pneumoniae* isolater (et serum resistent (391) og et serum følsomt (688)) blev undersøgt for involveringen af humane komplement regulatoriske proteiner i serum resistens. Resultaterne viste at mængden af C3 bundet til begge isolater var ens, men for isolat 391 var C3 kun bundet i kapslen, hvor det hurtigt blev nedbrudt til iC3b, i en proces det ikke involverede Faktor H. På trods af den hurtige inactivering af C3b, lykkedes det alligevel for komplement systemet at samle alle komponenter af MAC på isolat 391, dog i betragtelig mindre mængder end på isolat 688. Mængden af clusterin var højest på isolat 391, dog vidste IEM at clusterin primært var bundet i den ydre periferi af kapslen, og kunne derfor ikke være årsag til isolat 391's serum resistens. IEM viste yderligere at kapslen på 391 blev afskudt, i en proces der eksponerede en overflade under kapslen, som ikke bandt komplement komponenter. Calprotectin, et metalbindende protein med antimikrobielle egenskaber blev identificeret i store mængder på isolat 391. Calprotectin bundet til *K. pneumoniae* er en ny opdagelse, og effekten herf kendes derfor ikke. Helicobacter pylori kultiveret i medie supplementeret med calprotectin, viste modifikationer af Lipid A, en ændring i overfladespændingen og biofilmdannelse. Indikationer på en forskel i overfladespændingen mellem isolat 391 og 688, blev yderligere forstærket med proteiner identiferet på isolat 688. Her blev plasminogen, Factor V og properdin fundet i større mængder en på isolat 391, de tre proteiner er kendt for at binde til negativt ladede fosfolipider. Indikationer på en ubeskrevet bakteriel C3 konvertase blev set på isolat 688 og involverede hydrolyseret C3 (C3(H2O)), Factor B and properdin. Tilstedeværelsen af denne konvertase tilføjede yderligere til hypotesen om at serum resistens opstår om følge af en ændring i overfladespændingen.

Dette studie viste at C3b i kapslen på isolat 391 hurtigt blev nedbrudt til iC3b. Alle komponenter af MAC blev dog fundet sammen med clusterin på isolat 391. IEM viste dog at clusterin primært var bundet i den ydre periferi af kapslen, og ikke tæt på den ydre membran, og kunne derfor ikke redegøre for isolat 391's serum resistens. Indikationer på en forskel i overfladespænding blev observeret, denne forskel vil både kunne forklare de morfologiske ændringer i kapslen samt serum resistensen. Yderligere studier skal laves, for at bekræfte denne hypotese, samt calprotectins rolle i serum resistens såvel som vigtigheden af dannelsen af en konvertase indeholdende C3(H2O)

1 Introduction

1.1 *Klebsiella pneumoniae*

K. pneumoniae is a member of the Enterobacteriaceae family. It is a rod-shaped, non-motile, Gram negative bacteria, that primarily colonize the oropharynx and gastrointestinal tract in humans. *K. pneumoniae* can cause a wide range of infection, from urinary tract infections to pneumoniae and sepsis. The mortality rate infection by *K. Pneumoniae* is increasing due to the emergence of multidrug resistant strains, that limits the treatment options (Xu et al., 2017). The need for new therapeutics and further understanding of the pathogenesis of *K. Pneumoniae* is hence critically needed, as stated by the World Health Organization in 2017 (WHO, 2017).

K. Pneumoniae is encapsulated by a capsule composed by polysaccharides (CPS) (see Figure 1), that act as a virulence factor and can protect against phagocytosis. *K. Pneumoniae* is known to produce a cytotoxic extracellular toxic complex (ECT) composed primarily by capsule material and lipopolysaccharides (LPS) (Straus, 1987). LPS is major component in the outer membrane (OM) of Gram negative bacteria. It is composed by a Lipid A part, a core polysaccharide and O-antigen chain composed by repeating units of saccharides. The Lipid A part is located closest to the outer membrane and anchors the LPS to the bacteria. LPS also contributes to the structural stability of the outer membrane, due to inter-LPS ionic interaction, that cross-links neighboring LPS-molecules to each other by divalent ions (Vinogradov et al., 2002). Modifications to the Lipid A that reduces the negative charge of the outer membrane has been demonstrated to be highly correlated to colistin resistance (Kidd et al., 2017; Pragasam et al., 2017), and the modifications can be induced in a tissue-dependent manner in mice, suggesting that Lipid A modifications are induced in response to the extracellular environment (Llobet et al., 2015). The O-antigen of LPS is an oligosaccharide, a repetitive unit of 4-40 saccharides. The presence of the O-antigen characterizes the LPS type as smooth and LPS lacking the O-antigen is termed rough LPS. The composition of the O-antigen further sorts the LPS into different O-antigen serotypes (Vinogradov et al., 2002). The membrane of *K. Pneumoniae* consists of a inner membrane composed of a phospholipid bilayer, and outer membrane of phospholipids and Lipid A. In between the membranes is the periplamic space were a layer of peptidoglycan is found. In the outer membrane porins and outer membrane proteins are found, as well as pili here protrudes from.

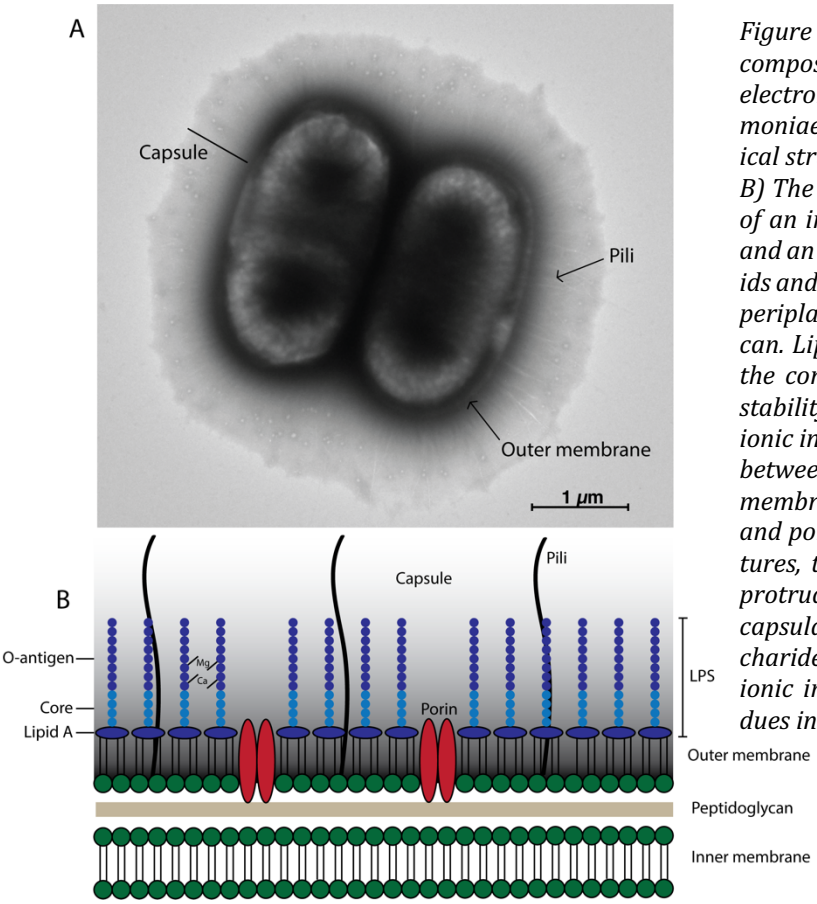

Figure 1. Morphological structure and membrane composition of K. pneumoniae. A) Transmission electron microscopic micrograph of two K. Pneumoniae, showing arrangement of the morphological structures capsule, pili and outer membrane. B) The membrane of K. pneumoniae is composed of an inner membrane of a phospholipid bilayer and an outer membrane composed of phospholipids and Lipid A. In between the two membranes in periplasmic space and a thin layer of peptidoglycan. Lipid A is also a part of LPS, through which the core and O-antigen of LPS is attached. The stability of the outer membrane is enhanced by ionic interactions by the divalent ions Mg and Ca, between neighboring LPS structures. In the outer membrane numerous outer membrane proteins and porins a present. Pili are long hairlike structures, that arise from the outer membrane and protrudes through the capsule. The capsule encapsulates the bacteria in a extracellular polysaccharide, and is attach to the outer membrane by ionic interactions with negatively charged residues in the LPS.

1.2 *K. pneumoniae* and serum resistance

A known and recognized virulence factor of *K. Pneumoniae* is its ability to survive direct complement mediated killing, yet the molecular mechanisms resulting in serum resistance remains unclear. Several studies have investigated the involved in this mechanism through the years. The capsule has been of great interest, early work done by Merino et al. showed that the capsule activates the complement system far from the outer membrane, but unencapsulated mutants remained serum resistant. Furthermore, they showed that serum sensitive strains lacking the O-antigen of LPS were serum sensitive and unencapsulated mutants with O-antigen type 1 was serum resistant (Merino et al., 1992). Álvarez et al demonstrated that isolates lacking the O-antigen could survive in serum, but a mutant producing less capsule was killed, concluding that the capsule is a major contributor to serum resistance (Álvarez et al., 2000). These conclusions have recently been put to a test. A study from 2017 by DeLeo et al. found that two isolates harboring the exact same capsule and O-antigen genes differed significantly in survival rates in different concentrations of serum. Most recently Loraine et al. tried to find a genetic correlation to serum resistance by whole genome sequencing of 164 clinical *K. Pneumoniae* isolates from hospitals in Thailand. Surveying a wide of membrane components, virulence and antibiotic genes, including capsule and O-antigen genes, as well as comparing serum resistance to the amount of capsule produced by the isolates, they were unable to determine any correlation to serum resistance, despite their comprehensive work (Loraine et al., 2018)

1.3 The complement system

The complement system is an essential part of the innate immune system, promoting recognition of microbial intruders resulting in opsonization for phagocytosis or direct killing by poreforming structures called the membrane attack complex (MAC). Furthermore, it communicates with the adaptive immune system, and is involved in the removal of cellular debris and hemostasis (Ricklin et al., 2010). The complement system consists of a number of circulating and surface bound proteins, that serves as substrates, enzymes and regulators of an extracellular proteolytic cascade, that produces a number of different mediators of different functions including inflammation, opsonization and direct killing of bacterial intruders. The following will focus on the parts of the complement system that is involved in recognition and killing of bacteria and how bacteria circumvent the direct killing of complement system.

Complement activation is following three pathways, that differs mostly in the initiation and merge functionally by the assembly of a C3-convertase that cleaves C3 to C3a and C3b (Ricklin et al., 2010). The classical pathway (CP), is primarily initiated by antibody recognition of the surface of the bacteria, this antibody-antigen complex is recognized by C1q (see Figure 2). In addition, C1q is also able to recognize bacteria in an antibody-independent fashion, as it also has affinity for some bacterial components, as porins and LPS species (Albertí et al., 1996; Roumenina et al., 2008). C1q is a part of the circulating C1-complex, which also includes C1r and C1s. C1r and C1s has both proteolytic properties. Upon binding of the C1-complex to the surface of the pathogen, a dramatic conformational change occurs. The conformational change is believed to occur, due to an exchange of Ca^{2+} ions from C1 complex to the binding site. This conformational change results in that C1r will be activated to cleave and activate C1s, which in turn will cleave the circulating components C2 and C4, to C2b and C4b, which together forms the classical C3-convertase (C4bC2b), which is anchored covalently to the bacterial surface by the thioester group of C4b. The lectin mediated pathway (LP), is initiated by pattern recognition molecules, including Mannan-binding lectin (MBL), collectins and ficolins. These molecules recognize carbohydrates associated with the bacteria. Upon this recognition, MBL-assosiated serine proteases (MASPs) are activated. MASP-1 is responsible for cleavage of C4 and activation of MASP-2, while MASP-2 cleaves both C2 and C4 into C2b and C4b. These will form a C3-convertase identical to the one formed by the classical pathway.

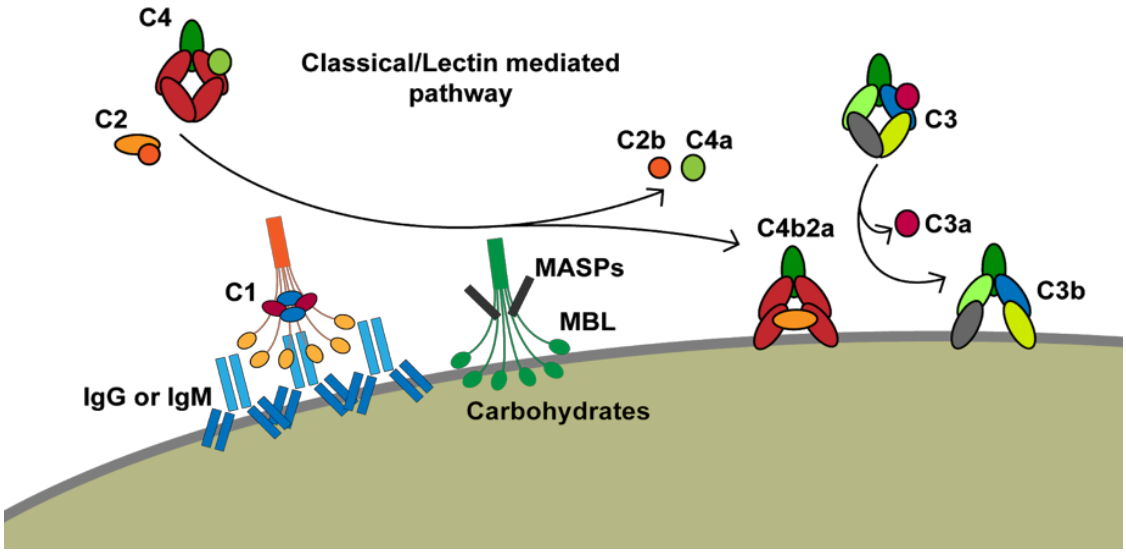

Figure 2. Classical and lectin pathway and C3-convertase assembly. The classical pathway uses IgG and IgM as pattern recognition molecules, for binding the C1-complex via the C1q. Once C1 has bound, C1r activates C1s, which have proteolytic properties on C2 and C4, cleaving them to release C2a and C4a. The resulting C4b and C2b forms the classical C3 convertase C4b2b. The lectin mediated pathway utilizes mannose binding protein (MBL), as patteren recognition molecules. MBL bind carbohydrates. Bound to MBL is MBL-associated serine proteaes (MASPs). MASP-1 cleaves C4 and activates MASP-2 to cleave both C2 and C4. The cleavages and the C3-convertase formed is identical to those of the classical pathway.

The alternative pathway (AP), differs significantly from the CP and LP (see Figure 3). It produces two different C3-convertases, one from spontaneously hydrolysis of the thioester group of C3, hydrolyzed C3 is termed C3(H2O). C3(H2O) binds Factor B (FB). C3(H2O)-bound FB will then be cleaved by Factor D (FD), releasing Ba and forming one of the alternative C3-convertase (C3(H2O)Bb)(Pangburn et al., 1981). The C3(H2O)Bb convertase is thought to mainly be present in the fluid phase, yet the formation of a surface bound C3-convertase involving C3(H2O), FB and properdin has been discovered on activated platelets (Saggu et al., 2013). The second C3-convertase produced by the AP is from preformed C3b that is covalently bound to the surface. This assembly also involves FB and FD, and results in the alternative C3-convertase C3bBb (Harboe & Mollnes, 2008).

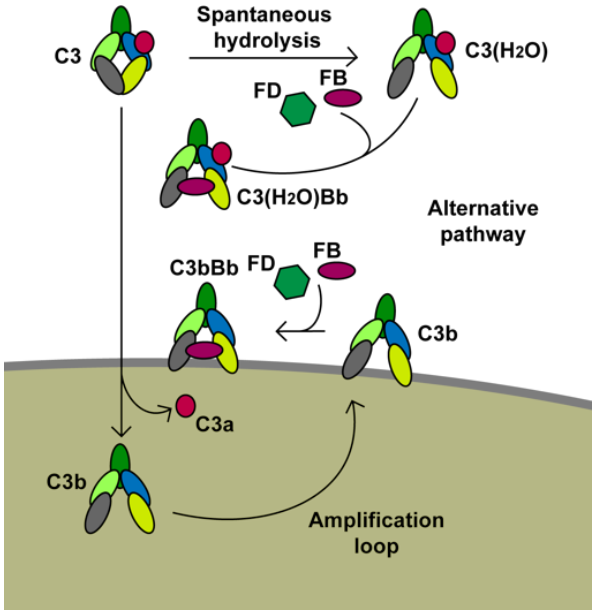

Figure 3. The alternative pathway C3-convertase assembly. The alternative pathway is spontaneous activated by hydrolysis of the thioester group of C3. This activation does not involve any proteolytic cleavages, but the conformational changes in C3 upon hydrylysis, give C3(H2O) C3b-like properties. Binding of Factor B, and activation of Factor B by Factor D forming Bb, gives the complex C3-convertase properties. Since the thioesther is hydrolyzed, the complex cannit bind covalently to surfaces, and is therefore active in the fluid-phase. The C3b formed in the fluid phase has a exposed and reactive thioester, and binds to surfaces, where it can form the surface bound C3-convertase C3bBb. Furthermore, Factor B and Factor B can form C3-convertases from C3b cleaved by the CP and LP, creating an amplification loop that rapidly enhance C3b deposition.

These C3-convertases cleaves circulating C3 into C3a and C3b. Upon cleavage, a conformational change of C3b occur, and a hidden thio-ester group becomes reactive, and C3b can hereby bind covalently to the bacterial surface (Gros et al., 2008). Here C3b can either enter the alternative pathway, and produce additional C3-convertases in an amplification loop, or it can bind to an existing C3-convertase to form the C5-convertase, C4bC2bC3b or C3bBbC3b.

The C5-convertase is the start of the Terminal Pathway (TP), the goal of which is to produce and integrate MACs into the membrane of the bacteria, leading to loss of integrity and hereby death (see Figure 4). The C5-convertase cleaves C5 into C5a and C5b. C5b then recruits complement components C6, C7, C8 and C9, which together form the MAC. The assembly takes place in an orderly manner, starting with C6 and C7. Once the lipophilic C5b-7 is formed, the complex has membrane binding properties. With the addition of C8, C5b-C8 is able to integrate and penetrate itself in and through the membrane. C9 is then recruited, multiple copies of C9 form a ring-like structure in the membrane (Hadders et al., 2012). This structure has pore-like properties, which allow uncontrolled passive transport across the membrane, leading to a dramatic osmocolloid change and death of the bacteria hereof.

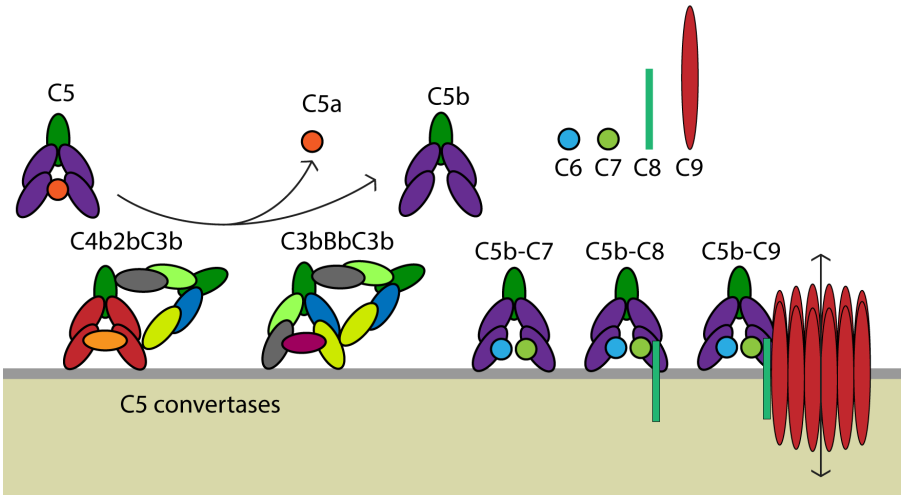

Figure 4. The terminal pathway. By the C5-convertases assembled by addition of C3b to the C3-contertases, C5 is cleaved to C5a and C5b. C5b has no binding properties, but recruit C6 and C7 to obtain those properties. Once C5b-C7 is formed the complex can bind to membranes. By addition of C8, the complex gains membrane penetrating properties, which is utilized to form a pore like structure by numerous copies of C9. The final structure, C5b-C9, allows passive transport across the membrane, which results in loss of integrity and the bacteria die of a dramatic osmocolloid change.

The separate pathways act in independence of each other in the initiating steps of recognition of the pathogen, yet the AP also acts as an amplifier of all pathways once C3b is formed and bound, hence the AP is responsible for 80% of the complement activity regarding pathogen elimination. A reason for that, is the positive regulator of the AP, properdin. Properdin stabilizes the AP C3-convertase, resulting in a significant increase of its half life, and protection from degradation by complement regulators (Fearon et al. , 1975), hence an increased production of C3b that can enter the amplification loop and/or produce C5-convertases. Furthermore, properdin can act as a recognition molecule, to initiate the AP on surfaces independently of the CP and LP. (Ferreira et al., 2010; Kimura et al. , 2008)

1.3 Regulation of complement activation

The complement system is not just activated upon pathogenic intruders, it also serves as an effective locator of cellular debris and is important for the maintenance of hemostasis. Therefor the complement system is highly regulated, to prevent damage of healthy self-tissue. Regulation takes place at all levels of complement activation and will be further explained in the following sections.

C1 inhibitor (C1Inh), is a regulator of the classical pathway. C1Inh binds to and inactivate C1r and C1s of the C1-complex. In addition, it detaches C1r and C1s from C1q, limiting activation of the CP. By inactivating of the C1-complex, the production of C4b and C2b will drop, and the classical C3-convertase will not be assembled (Davis III et al., 2010). Factor I is a serine protease found in plasma, it cleaves C3b to iC3b (see Figure 5), which then is unable

to bind Factor B, and the convertase activity is lost. Factor I has also inactivation properties against C4b, cleaving it to C4c and C4d, and hereby loss of convertase activity. Factor I has a number of cofactors, that is necessary for Factor I's proteolytic properties. Factor H and C4-binding protein are fluid phase cofactors necessary for cleavage of C3b and C4b respectively. The surface bound cofactors Complement receptor 1 (CR1), Membrane cofactor protein (MCP) and decay accelerating factor (DAF) are found on healthy self tissue, where they ensure fast degradation of both C3b and C4b, by acting as cofactors, resulting in a cleavage independent of Factor H (Merle et al., 2015).

The MAC is also highly regulated to prevent insertion to healthy tissues. The assembly has happen in right order and close to a membrane. C8 can act as a inhibitor, if it binds to the C5b-C7 complex prior to membrane binding. Furthermore, the products C5b-C7, C5b-C8 and C5b-C9 will be deactivated by clusterin or vitronectin, if they are not bound to a membrane. Clusterin and vitronectin blocks the hydrophobic part of the complexes, thus preventing them to bind and penetrate a membrane (Hadders et al., 2012).

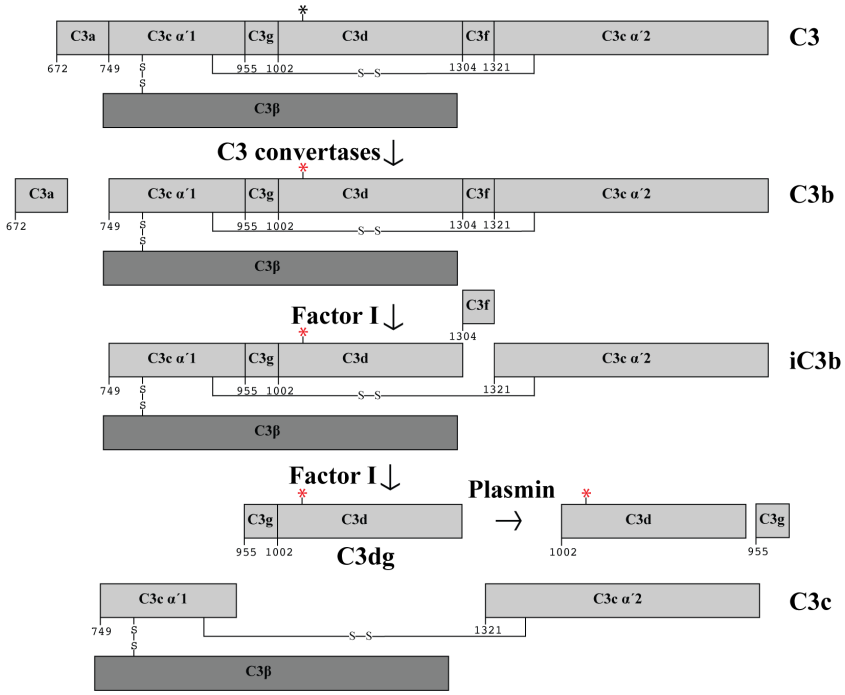

Figure 5. Proteolytic cleavages of C3. C3 circulates with a hidden thioesther (black star on C3d), and thus possess no binding properties. Once C3 is cleaved to C3b by a C3 convertase, a conformational change occurs and the thioester becomes reactive (red star). The first inactivating cleavage is the cleavage from C3b to iC3b, performed by Factor I in presence of cofactor Factor H, CR1, DAF or MCP. The cleavage of iC3b to C3dg is also facilitated by Factor I, but only in presence of a membrane bound cofactor (CR1, DAF or MCP). Plasmin is able to cleave C3dg to C3d and C3g.

Aim of the study

A study by colleges (Jensen et al.,)has shown a major difference in serum resistance of clinical isolates of *K. Pneumoniae* as well as morphological changes of the capsule of serum resistant isolates of *K. Pneumoniae*, after incubation in normal human serum (NHS). By immunoelectron microscopy they found that complement components only were deposited in the capsule on serum resistant isolates, and that a capsule shedding occurred, exposing a surface of the bacteria underneath the capsule that did not bind complement components. This study aims to determine the molecular background of the mechanisms involved to survive complement mediated lysis. The present research on the complement system relies on immunological methods and due to the complexity of the system, and immunological cross reactions between cleavage products, the complement cascade is notoriously difficult and laborious to follow. This study will utilize the sensitivity of *state-of-the-art* tandem mass spectrometry. To track the complement cascade, N-terminal labelling of peptides probes this method to follow the downstream cleavages of the complement components, to determine the resistance to complement mediated killing in *K. Pneumoniae*. Two isolates where selected in regard to their ability to survive complement mediated killing, isolate 391 which survives and thrives in NHS and isolate 688 which is rapidly killed in NHS (Jensen et al.).

2 Methods

2.1 Origin of *K. Pneumoniae* isolates

Two clinical isolates of *K. Pneumoniae*, 391 and 688, were provided by Henrik Carl Schønheyder, Department of Clinical Microbiology, Aalborg University Hospital. Isolates originates from blood cultures from patients admitted to Aalborg University Hospital between 2015 and 2017. Both patients suffered from a Hospital acquired infection and were immunocompromised either by medication or comorbidities.

2.2 Serum

Blood was obtained from a healthy male volunteer and prepared by a standard protocol. Heat inactivation of serum was performed by heating to 56 °C for 30 min. in a waterbath. The use of human serum was approved by the Regional Ethics Committee of Region Nordjylland (N-20150073).

2.3 Incubation of bacteria in human serum

Overnight cultures of each isolate in RPMI 1640 were used to inoculate a new culture in RPMI 1640, which was grown to an OD_{600} of 0.75 at 37 °C. 2.75 x 10^9 CFU was collected by centrifugation and washed in PBS. NHS or HIHS was added in a ratio of 1:1 with PBS, to a total volume of 300 µl, and gently mixed by pipetting. The bacteria were incubated in serum for 10 or 60 min at 37 °C. The bacteria were recollected by centrifugation and washed three times in PBS to remove any unbound serum proteins. For TEM and IEM, freshly incubated bacteria were stored on ice, and analyzed within hours. For MS-analysis bacteria was pelleted and kept at -80 °C until further processing.

2.4 Sample preparation for HPLC-MS/MS

2.4.1 Lysis

200 µl Lysis buffer (5.0% SDS in TEAB-buffer) was added to each sample. The sample where then; vortexed for 30 sec; heated to 95 °C for 5 min; ultrasonicated 10 x 30 sec at 50 W and reheated to 95 °C for 5 min, before centrifugation at 14,000g for 10 min. The supernatant hereof was then proceeded to further preparation, or stored at -80 °C.

2.4.2 Filter assisted sample preparation (FASP)

A FASP protocol was modified for N-terminal acetylation of cleaved peptides according to (Birkelund et al., 2009) Supernatant of lysed bacteria corresponding to 150 ug bacterial protein or 100 ug serum protein where transferred to a 30 kDa molecular weight cutoff spin filter, and the volume was increased to 200 µl using Digestion buffer (0.5% SDS in TEAB-buffer). Samples where then centrifuged at 14,000 g for 15 min, and the flow through

was discarded. 200 µl Digestion buffer was then added and centrifugation repeated. The samples were reduced and alkylated by 10 mM TCEP and 50 mM CAA in 200 ul Digestion buffer, the reaction went for 30 min at 37 °C. Samples were then washed twice in 200 µl Digestion buffer and centrifugation at 14,000 g for 15 min. The flowthrough was discarded. Samples for free amine acetylation labeling, were at this step incubated in 10mM sulfo-N-hydroxysuccin for 90 min at 30 °C. Acetylated samples were washed twice after the reaction in 200 µl Digestion buffer by centrifugation at 14,000 g for 15 min, to remove any residual sulfo-N-hydroxysuccin. Partial acetylation of serines and threonines was reverted by 1 µg hydroxylamine in 200 µl digestion buffer. Digestion of the samples were done by trypsin, in a concentration of 1 µg/100ug sample in 50 µl Digestion buffer. Proteins were digested overnight at 37 °C.

2.4.3 Peptide elution, ethyl acetate extraction and C18 purification

After digestion the samples were collected by centrifugation at 14,000 g for 15 min. Additional 100 µl TEAB buffer was added to the spinfilter, to maximise the elution of peptides. Centrifuged was repeated, and the peptide enriched flowtrough was collected. To remove residual organic solvents an ethyl acetate extraction was performed. Ethyl acetate was added in a ratio of 3:1 to sample volume and acidified by adding TFA to a final concentration of 1%. Samples were vortexed and centrifuged at 14,000g for 1 min to obtain phase separation. The top organic phase was then removed. This extraction was repeated three times. The final lower aquatic phase, containing the peptides, were then dried in a vacuum centrifuge and the peptides were resuspended and purified on a 100 µl Pierce C18 stagetip according to manufacturer's instructions (Thermo Scientific). The final purified peptides were dried in a vacuum centrifuge and stored at -80 °C until further analysis.

2.5 HPLC-MS/MS-analysis

Dry peptides were resuspended in 100 ul of 2% acetonitrile and 0.1% formic acid in water. Peptides were separated by reverse phase liquid chromatography on a Ultimate™ 3500 RSLCnano (Thermo Scientific) coupled to a Q Exactive™ HF-X Hybrid Quadrupole-Orbitrap™ (Thermo Scientific), using a trap column setup; peptides were loaded to a 2 cm C18 trap column (Thermo Scientific) and separated using a 75 cm analytical C18 reverse phase column (Thermo Scientific). Columns were kept at a constant temperature of 60 °C. The peptides were eluted with a gradient of 98% solvent A (0.1% formic acid) and 2% solvent B (0.1% formic acid in acetonitrile) from min 0 to 10. Solvent B was then increased to 50% on an 85 min ramp gradient, before solvent B was increased to 98% on a 6 min ramp gradient from. The system was then washed by lowering solvent B to 2% on a 1 min ramp and kept there for 17 min. This yields a total runtime of 120 min per sample. All was done at a constant flow rate of 300 µl/min. All solvents were MS-grade quality.

2.6 Bioinformatics

The raw files from the MS/MS analysis were searched against the Uniprot human reference proteome (UP000005640, total protein count: 20.231, downloaded 2018-26-01). The search was performed in MaxQuant

(v1.6.3.4)(Cox et al., 2014), with standard settings with following minor adjustments; allowance of three miss cleavages and a maximum of four of the following posttranslational modifications, per peptide. Fixed modification; carbamidomethyl (C). Variable modifications; oxidation (M), deamidation (NQ), acetylation (K) and acetylation (peptide N-term). A label-free quantification (LFQ) was performed to evaluate and normalize protein abundance between samples. All proteins and peptides are reported at a false discovery rate of 1%, employing a highly confident identification. (Cox et al., 2014)

2.7 Transmission electron microscopy and immunoelectron microscopy

Transmission electron microscopy (TEM) and immunoelectron microscopy were performed according to Nielsen et al. and Lausen et al. Five µL of bacterial suspension was mounted to a 400 mesh carbon coated, glow discharged nickel grid and left to adhere for 1 min. The samples were washed in one drop of PBS and negatively stained with one drop of 1% phosphotungstic acid (PTA) at pH = 7.0, before blotted dry on filter paper. For immunoelectron microscopy (IEM), grids were, after mounting of bacteria, incubated in either pAb anti-C3d (1:200), or pAb anti-clusterin (1:200) in 0.5% ovalbumin in PBS for 30 min at 37°C. The grids were washed in three drops of PBS and incubated for 30 min at 37°C in secondary antibodies: goat anti rabbit or goat anti mouse (BBI solutions) conjugated to 10 nm colloidal gold diluted 1:25 in 0.5% ovalbumin (Sigma-Aldrich). Grids were washed in three drops of PBS and negatively stained with one drop of 0.5% PTA at pH = 7.0, before blotted dry with filter paper. Electron microscopy was performed on a JEM-1010 electron microscope (JEOL, Tokyo, Japan) operating at 60 kV, coupled to an electron-sensitive CCD camera (KeenView, Olympus Soft Imaging Solutions GmbH, Münster, Germany). For size calibration, a grid replica with 2,160 lines/mm was used.

2.8 Statistical analysis

The output from MaxQuant was further analyzed using Perseus (v1.6.5.0). Pearson's correlation coefficients were calculated to evaluate reproductivity of technical replicates. To calculate and visualize significant differences in the abundance of human proteins bound to the two bacterial isolates, a two-sided t-test was performed, with an FDR at 0.05 and S0=0.1 and volcano plots of the results generated.

3 Results

3.1 Strength of methods to identify complement proteins

To evaluate the strength of the used method to detect complement components and related proteins, 2 ul fresh human serum was prepared and digested as stated in the methods section. The analysis yielded a total of 255 protein identifications, of which 28 are directly related to the complement system (see Table 1), alongside with 35 immunoglobulin components (not shown). These results confirm that it is possible to detect all complement components, and members of all the major regulators and initiators of all three pathways.

Complement components and related proteins identified in serum

Uniprot Acc.	Protein name	Gene name	Unique peptides	Mol. weight	Function
O75636	Ficolin-3	FCN3	3	32.90	Initiator – Lectin pathway
P02745	Complement C1q subcomponent subunit A	C1QA	3	26.01	Initiator – Classical pathway
P02746	Complement C1q subcomponent subunit B	C1QB	7	26.72	Initiator – Classical pathway
P02747	Complement C1q subcomponent subunit C	C1QC	6	25.77	Initiator – Classical pathway
P00736	Complement C1r subcomponent	C1R	20	80.12	Initiator – Classical pathway
Q9NZP8	Complement C1r subcomponent-like protein	C1RL	1	53.50	Initiator – Classical pathway
P09871	Complement C1s subcomponent	C1S	15	76.68	Initiator – Classical pathway
P06681	Complement C2	C2	10	83.27	C3/C5 convertase component
P01024	Complement component C3	C3	132	187.15	C3/C5 convertase component
P0C0L4	Complement component C4-A	C4A	4	192.78	C3/C5 convertase component
P0C0L5	Complement component C4-B	C4B	7	192.75	C3/C5 convertase component
P01031	Complement component C5	C5	57	188.30	MAC component
P13671	Complement component C6	C6	13	104.80	MAC component
P10643	Complement component C7	C7	15	93.52	MAC component
P07357	Complement component C8 alpha chain	C8A	10	65.16	MAC component
P07358	Complement component C8 beta chain	C8B	12	67.05	MAC component
P07360	Complement component C8 gamma chain	C8G	8	22.28	MAC component
P02748	Complement component C9	C9	16	63.17	MAC component
P00751	Complement factor B	CFB	38	85.53	Alt. convertase component
P00746	Complement factor D	CFD	2	27.03	Activates Factor B
P08603	Complement factor H	CFH	27	139.0	Negative regulator
Q03591	Complement factor H-related protein 1	CFHR1	1	37.65	Negative regulator
P05156	Complement factor I	CFI	10	65.75	Negative regulator
P05155	Plasma protease C1 inhibitor	SERPING1	20	55.15	Negative regulator
P00747	Plasminogen	PLG	34	90.57	Negative regulator
P27918	Properdin	CFP	2	51.28	Positive regulator
P07225	Vitamin K-dependent protein S	PROS1	9	75.12	Negative regulator
P04004	Vitronectin	VTN	13	54.31	Negative regulator
P10909	Clusterin	CLU	14	52.50	Negative regulator

Table 1. Complement components and related proteins identified in normal human serum. The analysis of 2 μl serum, identified a total off 255 proteins of which the 28 proteins listed in the table is directly related to the complement system. Within the 255 identified proteins were also 35 immunoglobulin components. The analysis confirms, that it is possible to detect all components of the complement system by the methods used.

Study design

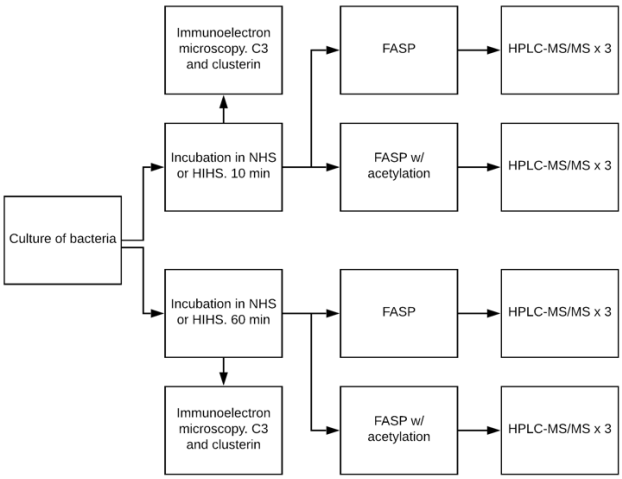

Figure 6. Flowchart of the study design. From a culture, same CFU of each isolate will be collected and incubated in either NHS or HIHS for 10 or 60 min. From here a small fraction of the samples will go to IEM, and the rest to FASP w/wo acetylation. Each sample from FASP will be run in triplicates on the HPLC-MS/MS. Each sample represent one biological replicate and 3 technical replicates. For IEM, only one technical replicate is performed. In total 16 samples will be analyzed by IEM, and 16 sets of triplicates, yielding 48 runs on the HPLC-MS/MS.

3.2 Reproducibility of HPLC-MS/MS analysis

As a validation of the technical reproducibility of the MS analysis, the intensities of quantifiable proteins were used to calculate the Pearson's correlation coefficient between replicates and scatterplots were generated and evaluated (see Figure 6). Perfect replicas will yield a coefficient of 1.0, and as all coefficients were in the range of 0.974 to 0.997, the quality of all the analyses is more than sufficient and all replicas were enrolled within the further data analysis. Calculations and scatterplots were generated in Perseus (v1.6.5.0)

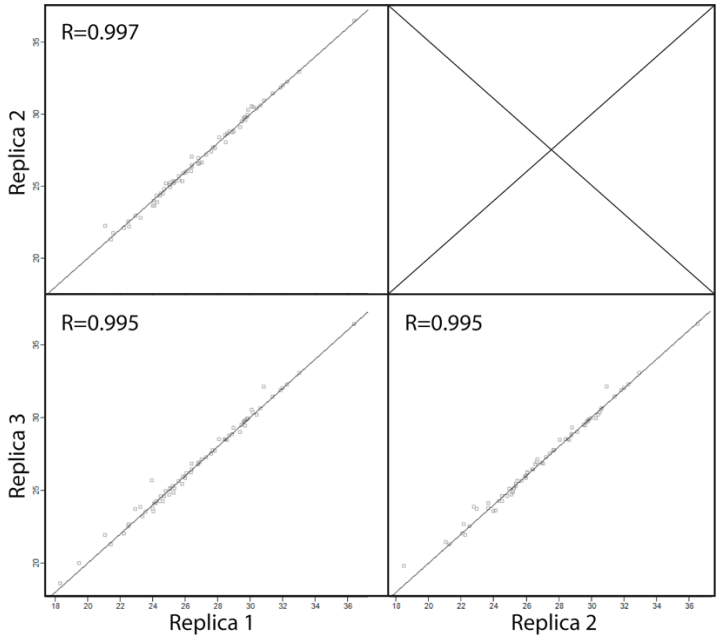

Figure 7. Scatterplots of protein LFQ-intensities to evaluate reproducibility of technical replicas. Here shown are representative scatterplots of isolate 688 after 60 min in NHS, showing intensities of proteins plotted against each other. The ideal replica yields a Pearson's correlation coefficient (R) of 1. Calculations and scatterplots were generated in Perseus (v1.6.5.0).

3.3 Abundance of human proteins

After incubation of bacteria in NHS for 10 or 60 min, the bacteria were thoroughly washed to remove on bound proteins, and whole bacteria with human proteins bound were analyzed by UHPLC-MS/MS and annotated by MaxQuant searching against the human reference genome. After filtration of contaminants, reverse hits and proteins only identified by site, a total of 32 and 87 quantifiable human proteins were identified after 10 and 60 min, respectively. Of the 32 proteins identified after 10 min, 12 proteins were significantly more abundant or uniquely found on isolate 688. 12 proteins were significantly more abundant or uniquely found on isolate 31. The remaining eight proteins were found on both isolates, but the abundance not significantly changed. Of the complement components and related proteins found, the abundance of C3, IgG2 and IgK, were equal between isolates. A change in abundance were observed for the rest of the complement related proteins; C4A, Factor B, IgG1, IgM were all found more abundant on isolate 688 and clusterin, C6, IgA1 and IgL1 were uniquely identified on isolate 688. For an overview over all proteins identified after 10 min, as well as foldchanges see Table 2.

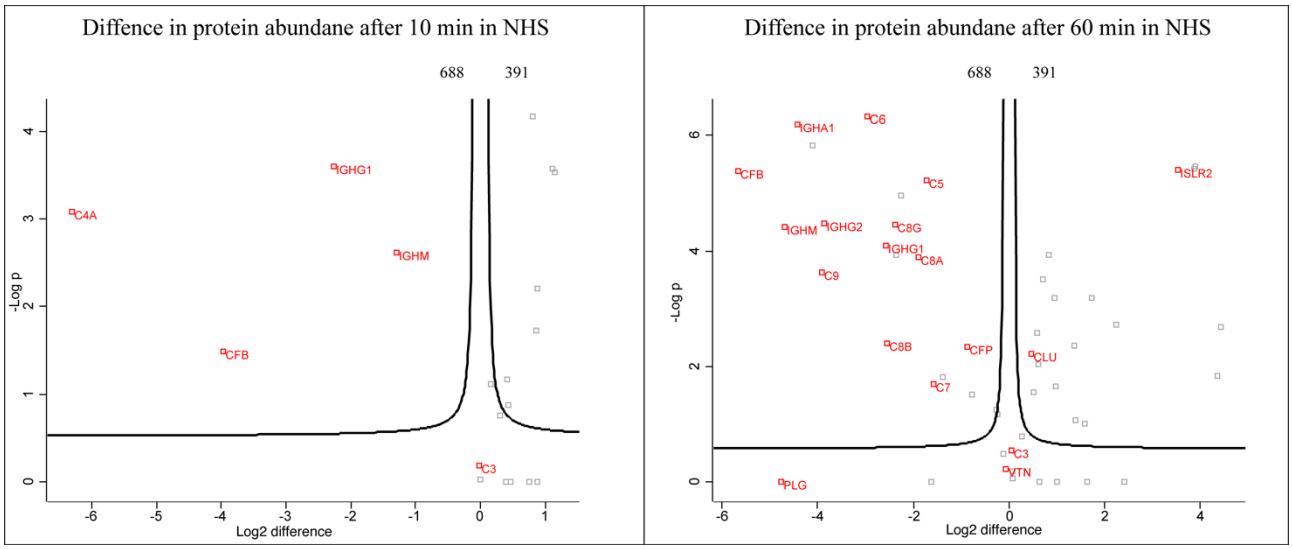

Figure 8. Volcano plots of quantifiable proteins found on both isolates. X-axis represents Log2 difference of the protein abundance, and the y-axis is the P-value of the change in -Log. At 10 minutes, evidence of C3-convertase assembly is observed by the presence of C4A and Factor B, despite the significant difference in the abundance of those C3-convertase proteins, the deposition of C3 is equal between isolates. At 60 min the difference in the abundance of C3 is still equal, but all the components of the MAC are highly more abundant on isolate 688. Of the complement related proteins, only the MAC-inhibitor clusterin is found more abundant on isolate 391.

Human proteins more abundant on isolate 688

Fold change	Uniprot Acc.	Protein name	Gene name	Unique peptides	Mol. weight	P-value
79.22	P0C0L4;P0C0L5	Complement C4-A; Complement C4-B	C4A;C4B	30	192.78	< 0.01
15.63	P00751	Complement factor B	CFB	27	85.53	0.03
4.80	P01857	Ig gamma-1 chain C region	IGHG1	3	36.10	< 0.01
2.46	P01871	Ig mu chain C region	IGHM	9	49.44	<0.01
Unique	P10909	Clusterin	CLU	4	52.50	
Unique	P13671	Complement component C6	C6	1	104.79	
Unique	P01876	Ig alpha-1 chain C region	IGHA1	4	37.65	
Unique	P0DOY3	Ig lambda-1 chain C regions	IGLC1	4	11.27	
Unique	O43866	CD5 antigen-like	CD5L	1	38.09	
Unique	P01023	Alpha-2-macroglobulin	A2M	5	163.29	
Unique	P02763	Alpha-1-acid glycoprotein 1	ORM1	1	23.51	
Unique	P02765	Alpha-2-HS-glycoprotein	AHSG	1	39.32	

Human proteins more abundant on isolate 391

Fold change	Uniprot Acc.	Protein name	Gene name	Unique peptides	Mol. weight	P-value
1.33	P04114	Apolipoprotein B-100	APOB	4	515.6	0.07
1.34	P02647	Apolipoprotein A-I	APOA1	9	30.78	0.13
1.76	P68871	Hemoglobin subunit beta	HBB	7	15.99	< 0.01
1.81	P54652	Heat shock-related 70 kDa protein 2	HSPA2	1	70.02	0.02
1.83	P08519	Apolipoprotein(a)	LPA	3	501.31	0,01
2.17	Q969S9	Ribosome-releasing factor 2, mitochondrial	GFM2	1	86.60	< 0.01
2.22	P02652	Apolipoprotein A-II	APOA2	2	11.18	< 0.01
Unique	A6NFN9	Protein ANKUB1	ANKUB1	1	47.66	
Unique	P01011	Alpha-1-antichymotrypsin	SERPINA3	3	47.65	
Unique	P06727	Apolipoprotein A-IV	APOA4	1	45.39	
Unique	Q96JN8	Neuralized-like protein 4	NEURL4	1	166.90	
Unique	Q9H6A9	Pecanex-like protein 3	PCNXL3	1	222.04	

Common human proteins

Fold change	Uniprot Acc.	Protein name	Gene name	Unique peptides	Mol. weight	P-value
Common	P01024	Complement component C3	C3	118	187.15	0.65
Common	P01834	Ig kappa chain C region	IGKC	5	11.77	0.08
Common	P01859	Ig gamma-2 chain C region	IGHG2	5	35.90	0.17
Common	A5D8W1	Cilia- and flagella-associated protein 69	CFAP69	1	105.88	0.94
Common	Q9Y697	Cysteine desulfurase	NFS1	1	50.19	1
Common	Q9H9P8	L-2-hydroxyglutarate dehydrogenase	L2HGDH	1	50.31	1
Common	P54819	Adenylate kinase 2	AK2	1	26.47	1
Common	Q6P4E1	Protein CASC4	CASC4	1	48.86	1

Table 2. Identified human proteins on isolate 391 ang 688 isolates after 10 min in normal human serum. The table lists the identified proteins, depending on their abundance on the isolates. Both significantly changed proteins and unique proteins are listed under the corresponding isolate. Proteins found on both isolates, but in equal abundance are listed under common proteins. The table shows the fold change, Uniprot accession, protein name, gene name, number of identified unique peptides, the molecular weight in kDa as well as the p-value of the change. Highlighted in dark grey are the significantly changed proteins and highlighted in light grey is the complement related proteins found uniquely or at equal abundance on the isolates.

Of the 87 human proteins identified after 60 min, 48 proteins were significantly more abundant or uniquely found on isolate 688. 25 proteins were significantly more abundant or uniquely found on isolate 31. The remaining 14 proteins were found on both isolates, but the abundance not significantly changed. Of the complement components and related proteins found, the abundance of C3, vitronectin and plasminogen, were equal between isolates. A change in abundance were observed for the rest of the complement related proteins; Factor B, IgM, IgA1, IgG2, IgG1, Properdin, C5, C6, C7, C8 and C9 were all found more abundant on isolate 688 and IgG3, IgG2, IgD, C1q, C4-binding protein, C1-inhibitor, Protein S, Factor H, Factor H-related protein 5, C4A, C4B were uniquely identified on isolate 688. On isolate 391, clusterin were the only complement related protein found significantly upregulated. For an overview over all proteins identified after 60 min, as well as foldchanges see Table 3.

No complement activation was observed on any of the isolates at 10 nor 60 min, when incubated in HIHS (data not shown).

Human proteins more abundant on isolate 688

Fold change	Uniprot Acc.	Protein name	Gene name	Unique peptides	Mol. weight	P-value
50.85	P00751	Complement factor B	CFB	23	85.53	< 0.01
25.79	P01871	Ig mu chain C region	IGHM	17	49.44	< 0.01
21.45	P01876	Ig alpha-1 chain C region	IGHA1	8	37.65	< 0.01
17.12	P02776	Platelet factor 4	PF4	11	10.85	< 0.01
14.94	P02748	Complement component C9	C9	14	63.17	< 0.01
14.53	P01859	Ig gamma-2 chain C region	IGHG2	7	35.90	< 0.01
7.79	P13671	Complement component C6	C6	26	104.79	< 0.01
5.93	P01857	Ig gamma-1 chain C region	IGHG1	9	36.11	< 0.01
5.81	P07358	Complement component C8 beta chain	C8B	11	67.05	< 0.01
5.18	P07360	Complement component C8 gamma chain	C8G	9	22.28	< 0.01
5.09	P0DOY2	Ig lambda-6 chain C region	IGLC6	1	11.29	< 0.01
4.75	P01834	Ig kappa chain C region	IGKC	8	11.77	< 0.01
3.71	P07357	Complement component C8 alpha chain	C8A	8	65.16	< 0.01
3.31	P01031	Complement component C5	C5	72	188.30	< 0.01

3.00	P10643	Complement component C7	C7	25	93.52	0.02
2.60	P01009	Alpha-1-antitrypsin	SERPINA1	5	46.74	0.02
1.82	P27918	Properdin	CFP	5	51.28	< 0.01
Unique	P01860	Ig gamma-3 chain C region	IGHG3	2	41.29	
Unique	P01877	Ig alpha-2 chain C region	IGHA2	1	36.59	
Unique	P01880	Ig delta chain C region	IGHD	2	42.35	
Unique	P02745	Complement C1q subcomponent subunit A	C1QA	1	26.02	
Unique	P04003	C4b-binding protein alpha chain	C4BPA	3	67.03	
Unique	P05155	Plasma protease C1 inhibitor	SERPING1	2	55.15	
Unique	P07225	Vitamin K-dependent protein S	PROS1	2	75.12	
Unique	P08603	Complement factor H	CFH	11	139.09	
Unique	P0C0L4	Complement C4-A	C4A	4	192.78	
Unique	P0C0L5	Complement C4-B	C4B	6	192.75	
Unique	Q9BXR6	Complement factor H-related protein 5	CFHR5	7	64.42	
Unique	O43866	CD5 antigen-like	CD5L	4	38.09	
Unique	P00450	Ceruloplasmin	CP	2	122.20	
Unique	P00738	Haptoglobin	HP	2	45.20	
Unique	P00739	Haptoglobin-related protein	HPR	2	39.03	
Unique	P01011	Alpha-1-antichymotrypsin	SERPINA3	5	47.65	
Unique	P01023	Alpha-2-macroglobulin	A2M	4	163.29	
Unique	P01042	Kininogen-1	KNG1	2	71.96	
Unique	P02749	Beta-2-glycoprotein 1	APOH	10	38.30	
Unique	P02751	Fibronectin	FN1	8	262.62	
Unique	P02790	Hemopexin	HPX	1	51.68	
Unique	P04114	Apolipoprotein B-100	APOB	1	515.60	
Unique	P04196	Histidine-rich glycoprotein	HRG	2	59.58	
Unique	P06396	Gelsolin	GSN	1	85.70	
Unique	P12259	Coagulation factor V	F5	11	251.70	
Unique	P18428	Lipopolysaccharide-binding protein	LBP	5	53.38	
Unique	P21333	Filamin-A	FLNA	2	280.74	
Unique	P27169	Serum paraoxonase/arylesterase 1	PON1	1	39.73	
Unique	P81605	Dermcidin	DCD	2	11.28	
Unique	Q96MT8	Centrosomal protein of 63 kDa	CEP63	2	81.34	
Unique	Q96PD5	N-acetylmuramoyl-L-alanine amidase	PGLYRP2	7	62.21	

Human proteins more abundant on isolate 391

Fold change	Uniprot Acc.	Protein name	Gene name	Unique peptides	Mol. weight	P-value
21.63	P05109	Protein S100-A8	S100A8	3	10.83	< 0.01
20,32	P06702	Protein S100-A9	S100A9	4	13.24	< 0.01
14.86	P54819	Adenylate kinase 2	AK2	1	26.48	< 0.01
14.58	Q969S9	Ribosome-releasing factor 2	GFM2	1	86.60	< 0.01
11.62	Q6UXK2	Immunoglobulin leucine-rich repeat protein 2	ISLR2	2	78.99	< 0.01
4.75	P69905	Hemoglobin subunit alpha	HBA1	10	15.26	< 0.01
3.32	P68871	Hemoglobin subunit beta	HBB	12	16.00	< 0.01
2.57	P63267	Actin	ACTG2	1	41.88	< 0.01
1.97	P02042	Hemoglobin subunit delta	HBD	1	16.06	< 0.01
1.93	P02655	Apolipoprotein C-II	APOC2	4	11.28	< 0.01
1.79	P02649	Apolipoprotein E	APOE	6	36.15	< 0.01
1.71	P02787	Serotransferrin	TF	3	77.06	0,03
1,63	P06727	Apolipoprotein A-IV	APOA4	9	45.40	< 0.01
1,52	P02774	Vitamin D-binding protein	GC	1	52.96	< 0.01
1,50	P02652	Apolipoprotein A-II	APOA2	6	11.18	< 0.01
1,43	Q86SG6	Serine/threonine-protein kinase Nek8	NEK8	1	74.81	0.03
1,39	P10909	Clusterin	CLU	8	52.49	< 0.01
Unique	P13929	Beta-enolase	ENO3	1	46.98	
Unique	P11021	78 kDa glucose-regulated protein	HSPA5	2	72.33	
Unique	P20700	Lamin-B1	LMNB1	1	66.40	
Unique	P29401	Transketolase	TKT	1	67.88	
Unique	P47756	F-actin-capping protein subunit beta	CAPZB	1	31.35	
Unique	P80188	Neutrophil gelatinase-associated lipocalin	LCN2	1	22.59	
Unique	P80511	Protein S100-A12	S100A12	1	10.57	
Unique	Q8IV04	Carabin	TBC1D10C	1	49.71	

Common human proteins

Fold change	Uniprot Acc.	Protein name	Gene name	Unique peptides	Mol. weight	P-value
Common	P01024	Complement component C3	C3	175	187.15	0.28
Common	P04004	Vitronectin	VTN	8	54.30	0.59
Common	P00747	Plasminogen	PLG	8	90.57	1
Common	P62937	Peptidyl-prolyl cis-trans isomerase A	PPIA	1	18.01	1
Common	P02656	Apolipoprotein C-III	APOC3	2	10.85	0.05
Common	P02766	Transthyretin	TTR	1	15.89	0.067
Common	P02647	Apolipoprotein A-I	APOA1	25	30.78	0.34
Common	P02730	Band 3 anion transport protein	SLC4A1	6	101.79	0.87
Common	P00734	Prothrombin	F2	14	70.04	0.64
Common	P02765	Alpha-2-HS-glycoprotein	AHSG	5	39.32	0.16
Common	P32119	Peroxiredoxin-2	PRDX2	2	21.89	1
Common	Q9Y490	Talin-1	TLN1	3	269.76	1
Common	P23528	Cofilin-1	CFL1	1	18.50	1
Common	P35579	Myosin-9	MYH9	1	226.53	1

Table 3. Identified human proteins on isolate 391 ang 688 isolates after 60 min in normal human serum. The table lists the identified proteins, depending on their abundance on the isolates. Both significantly changed proteins and unique proteins are listed under the corresponding isolate. Proteins found on both isolates, but in equal abundance are listed under common proteins. The table shows the fold change, Uniprot accession, protein name, gene name,

number of identified unique peptides, the molecular weight in kDa as well as the p-value of the change. Highlighted in dark grey are the significantly changed proteins and highlighted in light grey is the complement related proteins found uniquely or at equal abundance on the isolates.

3.4 C3 cleavage rates

Observing the MS/MS data on the level of proteins, it is clear that the regulation of the complement cascade takes place at the level of C3 in the complement cascade, as C3 abundance remained equally among the isolates between 10 and 60 min, but all the downstream complement components were more abundant on isolate 688. The following will investigate the structure and cleavage rates of C3.

By dividing the intensity of the N-terminal acetylated peptide, with the intensity of its unmodified counterpart a mod/base-ratio was calculated. Because of all endogenous cleavages of C3 is in a tryptic site, the N-terminal of a peptide will remain unmodified if the cleavage does not happen during serum incubation, whereas the N-terminal of a peptide cleaved under serum incubation will become acetylated during the sample preparations described in the methods section. With the mod/base-ratio it is therefore possible to track the cleavage rates of C3, and compare them between isolates to determine any difference in the structure of C3 bound to the isolates. Sulfo-N-hydroxysuccin acetylates all free amines, which are situated at all N-terminals and on lysine (K) residues. Furthermore, when lysine is modified by acetylation, trypsin loses its ability to cleave the peptide after this lysine, resulting in a missed cleavage. Both lysine acetylation and N-terminal yields a mass change of + 42.01 Da, making the modifications difficult to discriminate bioinformatically when a lysine residue is at the first position or is the first identified amino acid in a peptide. Therefore, a manual conformation and filtration of all N-terminal acetylation of C3 peptides was performed, based on the MS2 spectra. An N-terminal acetylation was accepted when the first amino acid was not a lysine or/and when the first identified amino acid was not a lysine. The reporting of mod/base-ratio will be based only on intensities of peptides identified in acetylated samples, whereas mapping of identified peptides is reported from both acetylated and non-acetylated samples.

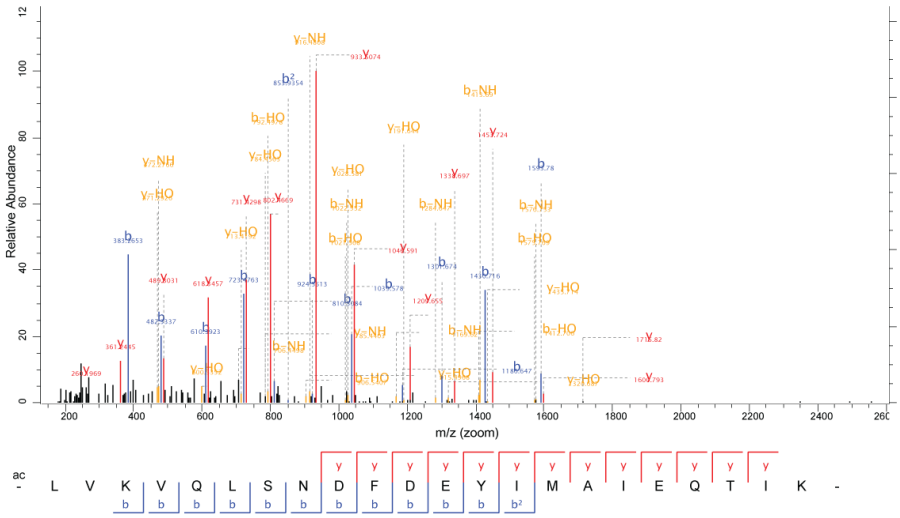

Figure 9. MS2 spectrum of a peptide with a non-accepted N-terminal acetylation. This peptide was not accepted because the first identified amino acid is a lysine. The mass change can therefore not be acknowledged as a N-terminal acetylation.

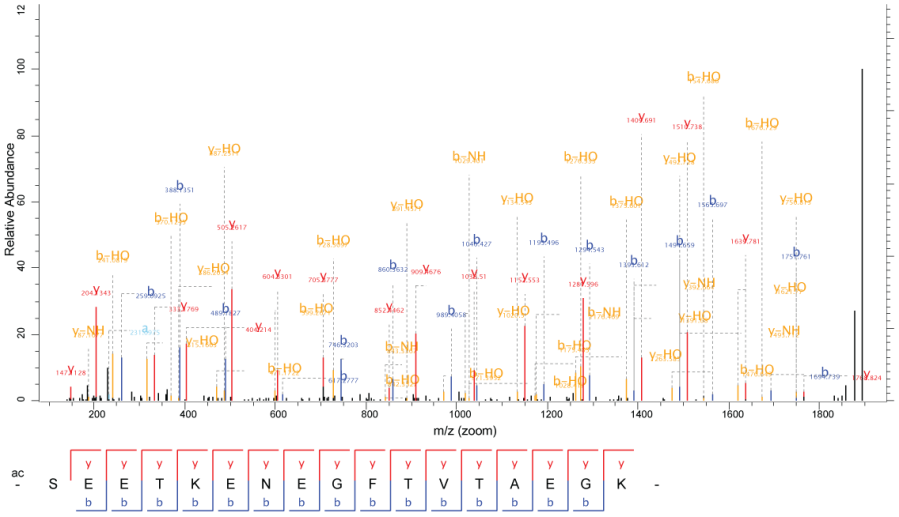

Figure 10. MS2 spectrum of a peptide with an accepted N-terminal acetylation. This peptide was accepted because it fulfilled the rules set for the acceptance of a N-terminal acetylation.

All accepted N-terminal acetylations were placed in the N-terminal of the known cleavage products of C3; Alpha'1, C3g, C3d and Alpha' 2. Cleavages are given roman numerals, depending on their placement in the C3 protein, starting from the N-terminal of the protein. Modifications of the search criteria of MaxQuant, such as allowance of semitryptic cleavages or number of additional missed cleavages and modification did not reveal other N-terminal acetylations of C3.

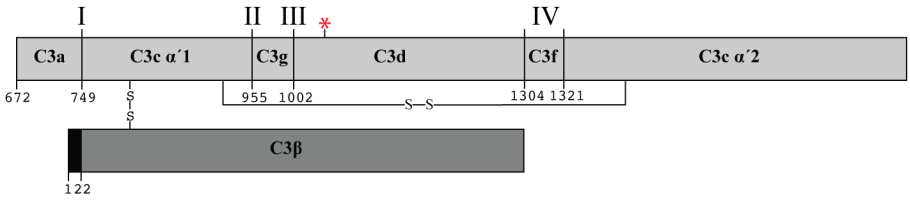

Figure 11. C3 cleavages and cleavage products, with inter- and intrachain disulfide bonds shown. Cleavages are designated a roman numeral for ease. Shown with numbers, are the position of the N-terminal amino acid of the following cleavage product. Marked with a red star, is the thioester group on C3d.

Ratios of modified N-terminals at cleavage I (see Figure 12). After 10 min in NHS, the mod/base-ratio of the N-terminal of Alpha'1 is high for both isolates, 25.99 for isolate 391 and 18.33 for isolate 688. A change is observed after 60 min in NHS, here the ratio for isolate 391 is even higher, but for isolate 688 it drops to 1.84. Peptides of C3a was only identified in serum samples.

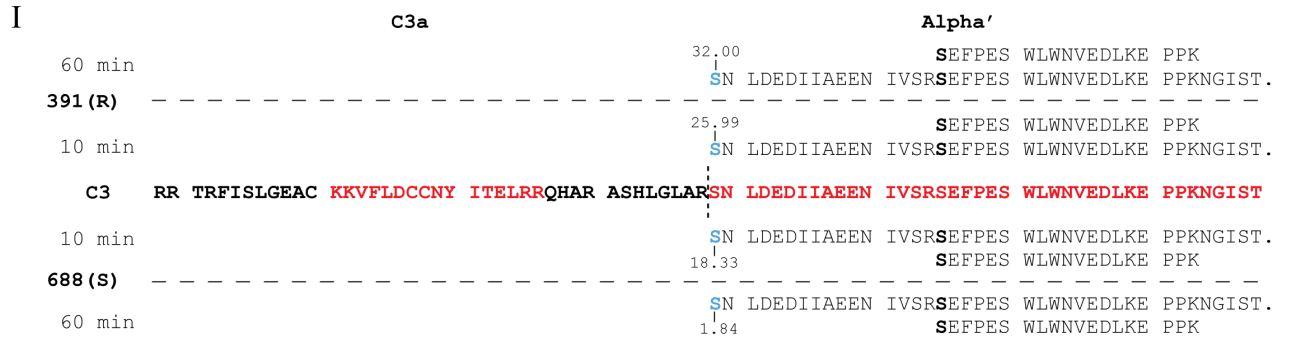

Figure 12. Mapping of identified peptides and their mod/base-ratio at cleavage I. The figure shows 40 amino acids on both sides of the cleavage, shown in bold black and red. Highlighted in red are the peptides identified in serum. The N-terminal amino acid in the cleavage site are highlighted in blue, and the mod/base-ratio shown in numbers in association to that amino acid. The mod/base-ratio is calculated by dividing the intensity of the N-terminally acetylated peptide by the intensity of the unmodified peptide. At 10 min the mod/base-ratio are high for both isolates, 391; 25.99 and 688; 18.33. At 60 min the ratio is even higher for isolate 391 but drops to 1.84 for isolate 688. Mappings of the identified peptides are similar for the isolates at both times, and peptides of C3a is only identified in serum. Bold letters in the mappings indicate the N-terminal of a new peptide. Dots at the end or start of the mapped peptides indicate, that the length of the peptide extends further than the shown sequence of C3.

Ratios of modified N-terminals at cleavage II (see Figure 13). Acetylation of N-terminals was not observed after 10 min in NHS. At 60 min, the mod/base-ratios were low, 0.01 for isolate 688 and 0.02 for isolate 391. Furthermore, peptides extending over the cleavage sites were also identified.

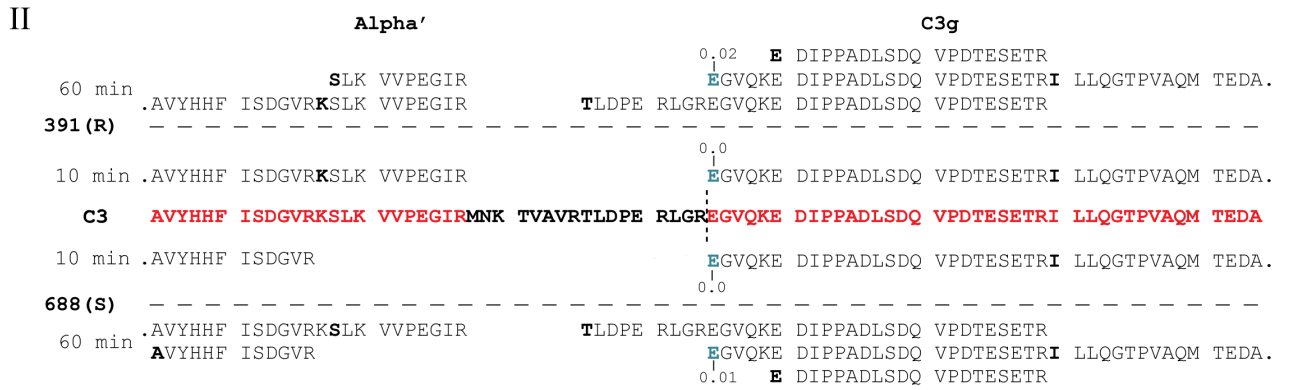

Figure 13. Mapping of identified peptides and their mod/base-ratio at cleavage II. The figure shows 40 amino acids on both sides of the cleavage, shown in bold black and red. Highlighted in red are the peptides identified in serum. In the mappings, the N-terminal amino acid in the cleavage site are highlighted in blue, and the mod/base-ratio shown in numbers in association to that amino acid. The mod/base-ratio is calculated by dividing the intensity of the N-terminally acetylated peptide by the intensity of the unmodified peptide. At 10 min no N-terminal acetylation was identified. At 60 min, N-terminal acetylation was observed, yet in small quantities; 0.02 for isolate 391 and 0.01 for

isolate 688. Mappings of the identified peptides are similar for the isolates at both times. To be noticed, is the peptides extending over the cleavage site at 60 min. Dots at the end or start of a mapped peptide indicate, that the length of the peptide extends further than the shown sequence of C3.

Ratios of modified N-terminals at cleavage III (see Figure 14). Acetylation of N-terminals was not observed after 10 or 60 min in NHS. The first peptide of C3d harbors the thioester group of C3, and two different modification states was observed for this peptide, and the amino acids forming the thioester group; the cysteine (C) at position 1010 and the glutamine (Q) at position 1013. At 10 min a common modification was observed; carbamidomethylation (CAM) of C and deamidation of Q. At 60 min the common specie of this peptide was also identified on both isolates, but on isolate 688 a new modification status of the peptide is identified, resulting in a mass shift of +128.478 Da. The exact structure of the modification could not be determined. The unknown modification was present in both acetylated and not acetylated samples of isolate 688, indicating that the modification was not produced by sulfo-N-hydroxysuccin.

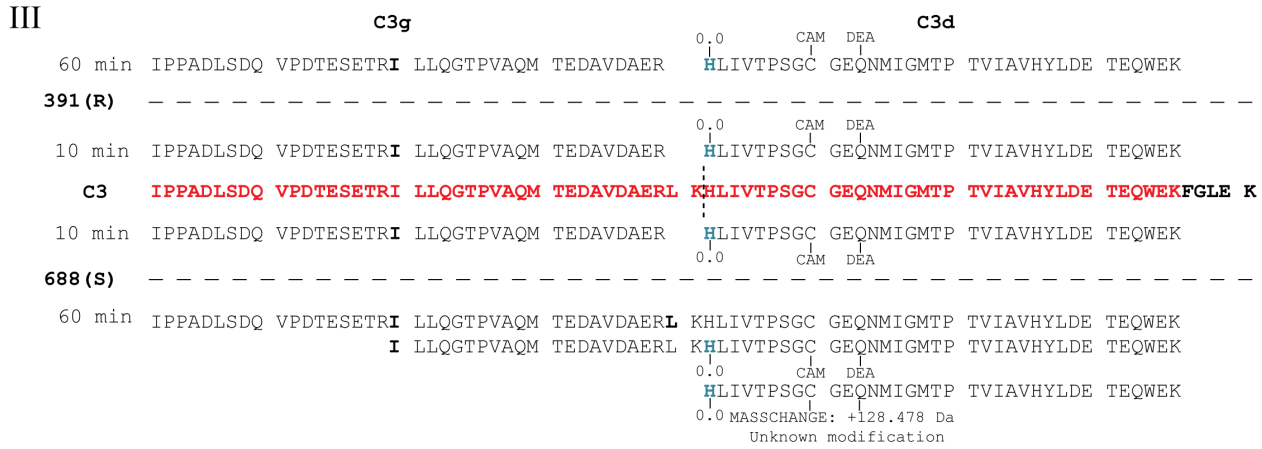

Figure 14. Mapping of identified peptides and their mod/base-ratio at cleavage III. The figure shows 40 amino acids on both sides of the cleavage, shown in bold black and red. Highlighted in red are the peptides identified in serum. In the mappings, the N-terminal amino acid in the cleavage site are highlighted in blue, and the mod/base-ratio shown in numbers in association to that amino acid. The mod/base-ratio is calculated by dividing the intensity of the N-terminally acetylated peptide by the intensity of the unmodified peptide. N-terminal acetylation was not observed at any time. The first peptide of C3d harbors the thioester group of C3, and different modification states of this peptide was observed on the isolates, in relation to the amino acids forming the thioester group, cysteine at position 1010 and glutamine at position 1013. At 10 min both isolates shared a peptide, with a carbamidomethylation (CAM) on the cysteine (C) and a deamidation (DEA) of the glutamine (Q). After 60 min this shared peptide were identified on both isolates, but on 688 a secondary modification state of the peptide was identified, causing a mass shift of 128.47 Da.

Ratios of modified N-terminals at cleavage IV (see Figure 15). At min 10, the mod/base-ratio showed a great difference, with 104.36 on isolate 319 and 1.22 on isolate 688. At 60 min the only unmodified N-terminal peptides of alpha'2 was identified on isolate 391, yet only at very sparse intensities. Regarding isolate 688, the mod/base-ratio was increased to 12.25 after 60 min. Peptides of C3f was only identified on isolate 688 after 60 min.

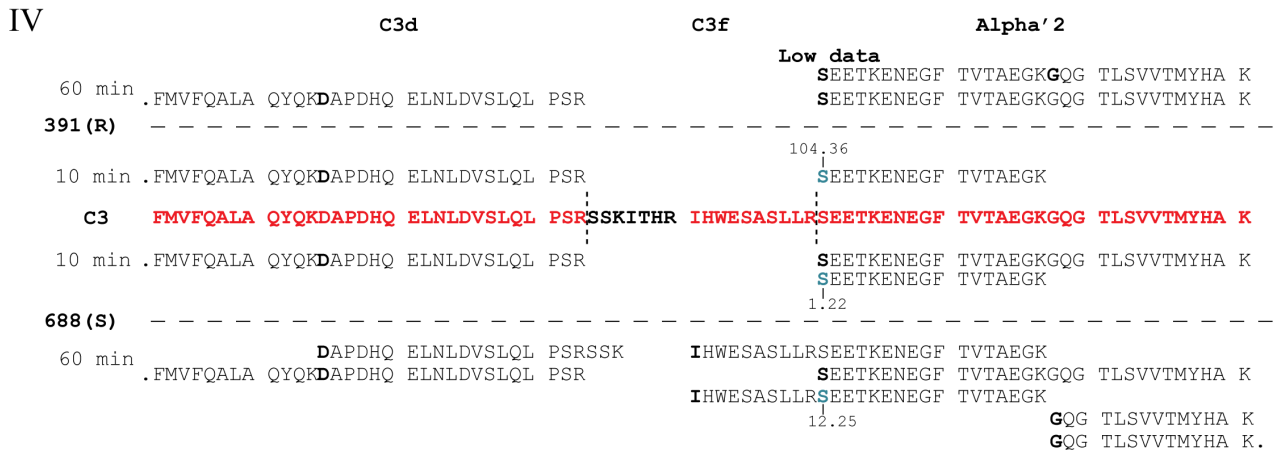

Figure 15. Mapping of identified peptides and their mod/base-ratio at cleavage IV. The figure shows 40 amino acids on both sides of the cleavage, shown in bold black and red. Highlighted in red are the peptides identified in serum. In the mappings, the N-terminal amino acid in the cleavage site are highlighted in blue, and the mod/base-ratio shown in numbers in association to that amino acid. The mod/base-ratio is calculated by dividing the intensity of the N-terminally acetylated peptide by the intensity of the unmodified peptide. At 10 min a great difference in N-terminal acetylation was observed, with a mod/base-ratio of 104.36 on isolate 391 and 1.22 on isolate 688. At 60 min, N-terminal acetylation was not observed on isolate 391, and the identified unmodified peptides were only found at very low intensities. Regarding isolate 688, the mod/base-ratio increased to 12.25 after 60 min. Peptides of C3f were only identified on isolate 688 after 60 min. Dots at the end or start of a mapped peptide indicate, that the length of the peptide extends further than the shown sequence of C3.

3.4 Immunoelectron microscopy

3.4.1 Deposition of C3

Since a difference in C3 cleavage rates, and abundance of clusterin was observed in the MS-data, immunoelectron microscopy was performed to visualize the deposition of these proteins on the bacteria. Freshly serum-incubated bacteria were mounted to grids and labelled with primary antibodies to either C3 or clusterin. Gold-conjugated secondary antibodies were then added, enabling the localization of C3 and clusterin to be visualized using electron microscopy. C3 deposition was investigated after 10 and 60 min, whereas deposition of clusterin only were investigated after 60 min.

Deposition of C3 at 10 min in NHS is shown in Figure 16 and was different on the two isolates. Micrographs of isolate 688 showed both bacteria that were lysed and bacteria that still had remained some of its structure of the outer membrane, assessed by the completeness of outer periphery of the outer membrane. C3 deposition was

found on both the outer membrane as well as in the capsule. All bacteria were found with fully or partly lost capsules. Micrographs of isolate 391 showed only bacteria that still had complete outermembranes, with a heavily deposition of C3 in the capsule, that was partly shedded or completey missing. No C3 deposition was observed on areas of the bacteria, where the capsule was missing. Micrographs of bacteria incubated in HIHS showed bacteria with complete outer membranes, and no C3 deposition.

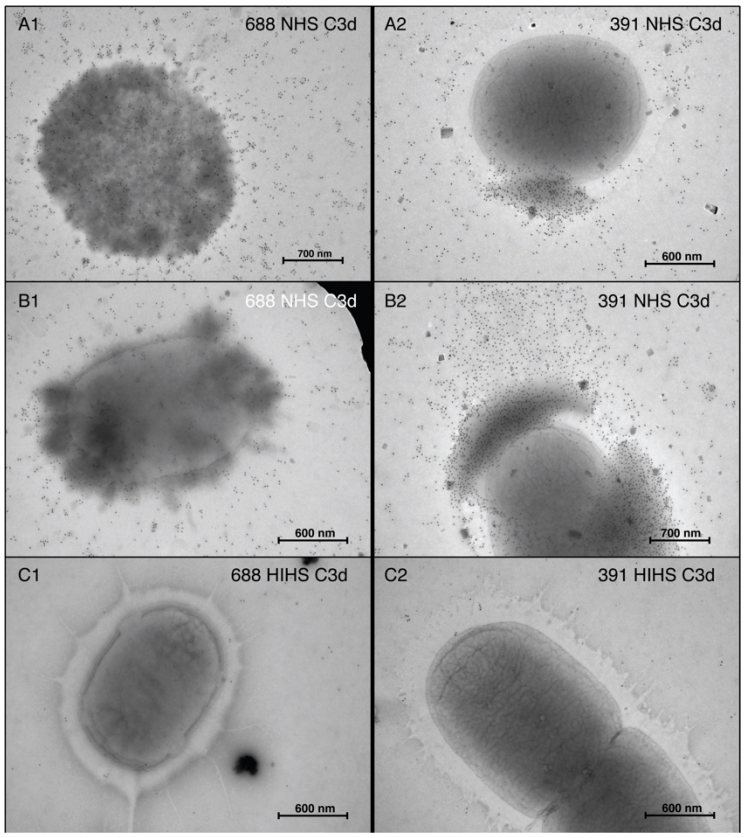

Figure 16. Micrographs of isolate 688 and 391 after 10 min in NHS or HIHS, labelled with primary anti-C3d and secondary 10 nm gold-conjugated antibodies. A1-B1: Micrographs of isolate 688, showing both lysed (A1) and complete bacteria (B1). Deposition of C3 is seen both on the outer membrane, as well as in the capsule.
A2-B2: Micrographs of isolate 391, showing only complete bacteria. Heavily deposition of C3 is seen only in the capsule of this isolate. No C3 deposition is seen in areas of the bacteria that are exposed, when the capsule is shedded of.
C1-C2: Micrographs of isolate 688 and 391 after 10 min I HIHS. Only complete bacteria, with no C3 deposition.
Scalebars in the bottom right corner of each micrograph, is produced by the use of a 2,160 lines/mm size replica.

Deposition of C3d after 60 min in NHS is shown in Figure 17. At 60 min all micrographs of isolate 688 showed lysed bacteria. The deposition of C3d was localized to still adherent capsule, outer membrane remains and bacterial fragments throughout the micrographs. Isolate 391 showed still fully complete outer membranes, and the deposition of C3d was only occurring in parts of the capsule that still were attached to the bacteria. At areas of the bacteria exposed by the capsule shedding, no binding of C3d occurred. No binding of C3d was observed on bacteria incubated in HIHS for 60 min.

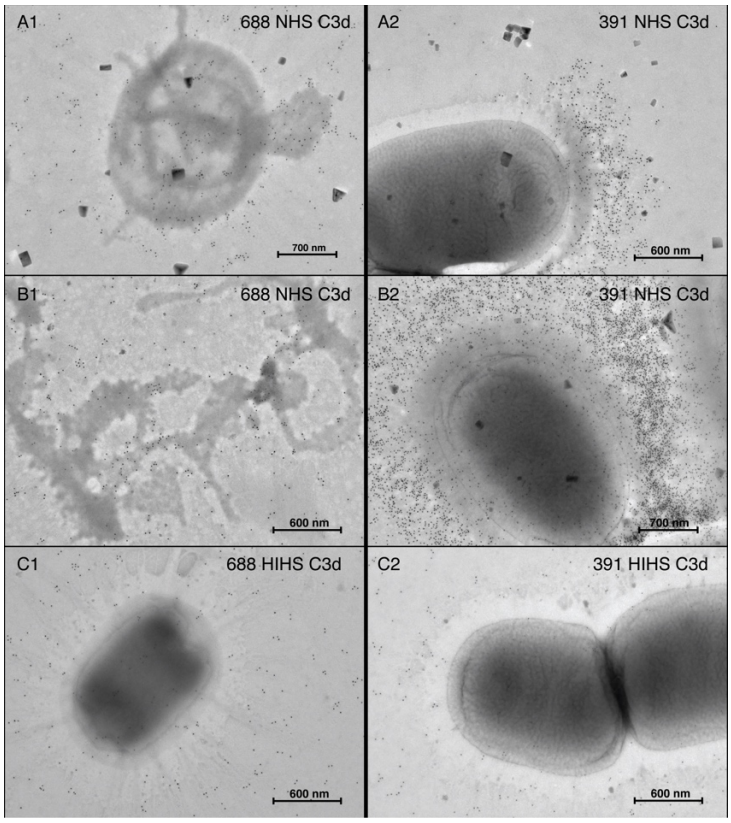

Figure 17. Micrographs of isolate 688 and 391 after 60 min in NHS or HIHS, labelled with primary anti-C3d and secondary 10 nm gold-conjugated antibodies. A1-B1: Micrographs of isolate 688 showing both lysed (A1 and B1) Deposition of C3 is seen both on the brokon outer membrane, as well as in the capsule still adherent to the bacteria. C3d was also seen bound to bacterial fragments throughout the micrographs.
A2-B2: Micrographs of isolate 391, showing only complete bacteria. Heavily deposition of C3 is seen only in the capsule of this isolate. No C3 deposition is seen in areas of the bacteria that are exposed, when the capsule is shedded of.
C1-C2: Micrographs of isolate 688 and 391 after 60 min in HIHS. Only complete bacteria, with no C3 deposition.
Scalebars in the bottom right corner of each micrograph, is produced by the use of a 2,160 lines/mm size replica.

3.4.2 Deposition of clusterin

Deposition of clusterin after 60 min in NHS (see Figure 18). The deposition of clusterin on the isolates was investigated, to determine whether clusterin could be involved in the inhibition of MAC formation in the outer membrane. Micrograpghs of isolate 688 showed overall sparse clusterin deposition, primarily in relation to the capsule. Micrographs of isolate 391 showed, compared to isolate 688, more deposition of clusterin. As the deposition was mostly seen in the outer parts of the capsule, the higher abundance of clusterin on isolate 391 is rather a consequence of MAC assembly in the capsule and subsequently binding of clusterin, than a recruiting mechanism developed by the bacteria to prevent MAC binding and insertion in the membrane.

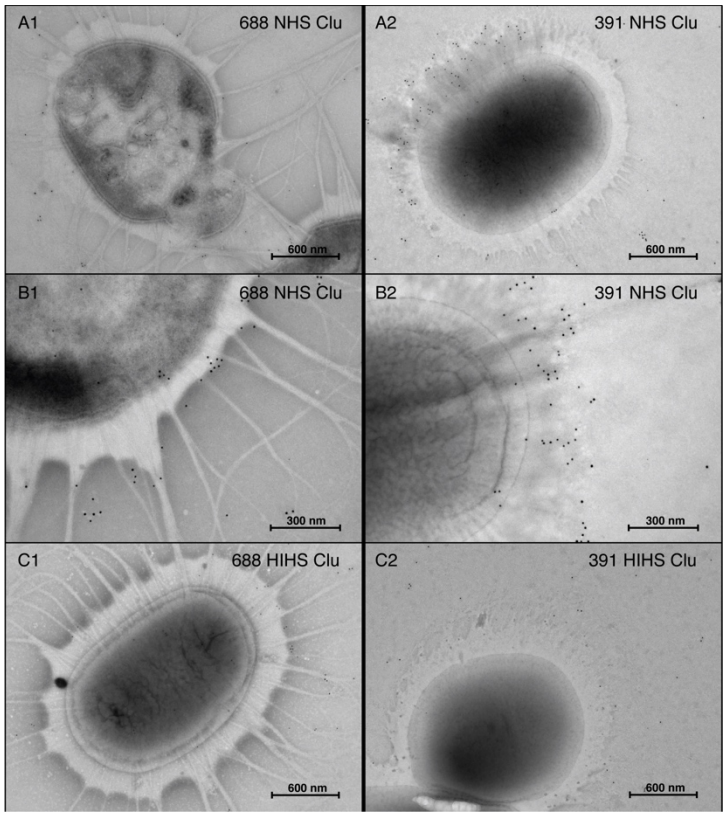

Figure 18. Micrographs of isolate 688 and 391 after 60 min in NHS or HIHS, labelled with primary anti-clusterin and secondary 10 nm gold-conjugated antibodies. A1-B1: Micrographs of isolate 688 showing both lysed bacteria (A1 and B1), with small qunatities of detected clustering, primary deposition of clusterin in the capsule. Few gold beads were observed in relation to the outer membrane.
A2-B2: Micrographs of isolate 391, showing only complete bacteria. More clusterin detected on this isolate, compared to 688. Clusterin is primarily seen in the capsule of this isolate, with only few gold beads in relation to the outer membrane. No clusterin deposition is seen in areas of the bacteria that are exposed, when the capsule is shedded of.
C1-C2: Micrographs of isolate 688 and 391 after 60 min in HIHS showed only complete bacteria, with no clusterin deposition.
Scalebars in the bottom right corner of each micrograph, is produced by the use of a 2,160 lines/mm size replica.

4 Discussion

Complement deposition

The abundance of complement related proteins differed significantly between the two isolates, while difference in C3 abundance remained unchanged, the abundance of initiators and MAC components where significantly favored isolate 688. This demonstrate that C3 deposition was independent of the abundance of initiating components, and thus only a low initiation is required to opsonize the bacteria with C3b. The presence of MAC-components on both isolates suggest that the complement cascade is able to produce and assemble MAC's on both isolates, yet in significantly higher amounts on isolate 688. MAC-assembly on serum resistant isolates of *K. pneumoniae*, that has no lytic effect on the bacteria, has previously been described by colleges and others (Jensen et al., 2019) and (DeLeo et al., 2017). Clusterin, an inhibitor of the insertion of MAC into membranes, was found more abundant on isolate 391 at 60 min. Recruiting of clusterin has previously been described for *Pseudomonas aeruginosa*, where it inhibited MAC assembly (Hallström et al., 2015). IEM micrographs of isolate 391 showed that clusterin only where present in the outer parts of the capsule, therefore the site of action was not on the outer membrane, and the mechanism of recruiting clusterin to the outer membrane as a inhibition of MAC, was rejected as a possible explanation to why isolate 391 survive direct complement mediated lysis.

C3 degradation rates

The mod/base-ratio of the C3a cleavage (I), was high for both isolates at 10 min, indicating a high percentage of the bound C3 was cleaved at this site, and thus initially bound in the form of C3b produced by the initiating mechanisms or the amplification loop of the alternative pathway, indicated by the presence of Factor B on both isolates. The first degradation cleavage of C3b is the cleavage that releases C3f (IV). At 10 min the mod/base-ratios showed a rapid cleavage rate and inactivation of C3b to iC3b on isolate 391, and a minor inactivation on isolate 688. The remaining two cleavage sites II and III, did not show any N-terminal acetylation at 10 min. Micrographs showing deposition of C3 on the isolates at 10 min, showed that C3 only where present in the capsule of isolate 391 and both in the capsule as well as on the outer membrane of isolate 688. This suggest that C3b bound in the capsule undergoes rapid inactivation, and the difference in mod/base-ratio can be explained by the fact that C3 also was bound to the outer membrane of 688 at this time, where inactivation rates is suggested to be different. The data did not show any known C3 regulators bound to isolate 391 at 10 min. Factor I or Factor H is known for facilitating the cleavage of C3b to iC3b, where Factor H acts as a cofactor for Factor I, yet Factor I's ability to facilitate this cleavage without prior Factor H binding has been determined previously (Cunnion et al., 2004), which can explain why binding of Factor H is not observed. The difference in inactivation is consistent with the difference in abundance of Factor B, which also will detach when C3b is cleaved to iC3b (Alcorlo et al., 2011). At 60 min a change in mod/base-ratio for cleavage I is observed, while it remained high on isolate 391, the ratio dropped dramatically for isolate 688. This indicates that the C3 bound to isolate 688 still has C3a attached, and has bound in form of C3(H2O). C3 convertases assembled with C3(H2O) is thought to only be active in the fluid phase, as the hydrolysis breaks the tioesther group, and therefore diminishes C3(H2O)'s ability to bind directly to surfaces. The assembly

of a surface bound C3-convertase involving C3(H2O) has been described on activated platelets, by utilizing properdin as a pattern recognition molecule. The kinetics of the assembly of the C3(H2O),FactorBb, properdin (C3(H2O)BbP) convertase was shown to only occur on the activated platelets, when properdin was the first component to be added to the platelets. It even out favored the formation of traditional C3bBbP (Saggu et al., 2013). By production of convertases with properdin, properdins protective role against degradation is also utilized as evidenced at the C3f cleavage (IV), the mod/base-ratio on isolate 688 did increase from 10 to 60 min, but at 60 min peptides extending over the cleavage site at both sites of C3f was identified, evidencing that bound C3 still had C3f attached and therefore active convertases was present. At cleavage III, the cleavage between C3g and C3d, no acetylation was observed after 60 min. Yet, different internal modification states of the first peptide of C3d was observed. The first peptide of C3d harbors the thioester group, and the different modification states of this peptide is hypothesized to be a consequence of the hydrolyzation. Yet, the data analysis used in this study could not identify the exact modification to confirm the hypothesis.

Work done by Holt et. al has demonstrated that properdin binds to negatively charged polyanionic structures (Holt et al., 1990), indicating that surface charge is essential for properdin binding. The finding of plasminogen and Factor V on isolate 688, further demonstrates a difference in accessibility of negatively charged residues, as they also binding the negatively charged phospholipids. If the assembly of C3-convertases on the outer membrane can utilize or are dependent on properdin as a platform for assembly, then the surface charge of the bacterial outer membrane becomes of great interest.

The surface exposed under the capsule of isolate 391 did not bind C3, and thus must the major reason why isolate 391 survives in serum. The outer membrane of *K. Pneumoniae* is covered in LPS, that is commonly known to be negatively charged, mainly due to the Lipid A part. Lipid A modifications of *K. Pneumoniae*, that reduces the negative charge of LPS, has been described in the context of resistance to polymoxins, which are small kationic antimicrobial peptides, which mechanism of action is to destabilize the outer membrane, by rearranging inter-LPS ionic interaction and insertion of a hydrophobic segment in the outer membrane which results in loss of membrane integrity and death of the bacteria because of uncontrolled passive transport across the membranes (Kidd et al., 2017; Yu et al., 2015). A mechanism which in many ways resembles the mechanism of the MAC, and thus Lipid A modifications may interfere with complement binding and insertion of the MAC in the outer membrane. By studying synthetic lipid bilayers Yorulmaz et al. showed that the surface charge of a lipid bilayer has to be negatively charged, for MAC assembly. MAC assembly was not observed on neutral or positively charged lipid bilayers. (Yorulmaz et al., 2015)

On isolate 391 three proteins of the Protein 100S family were found at high fold changes or uniquely on this isolate. Protein S100-A8 and A9 circulates the blood in a heterodimeric complex called calprotectin. Calprotectin has a variety of functions in the immune system. It has an antimicrobial mechanism by sequestering of iron, zinc and manganese, and thus reducing the access to these essential micronutrients for the bacteria (Nakashige et al, 2016). Binding of calprotectin can therefore be a source of these micronutrients, and add to knowledge how some isolates of *K. Pneumoniae*, thrive in serum. Furthermore, but mildly interesting in this settings is that culturing of

Helicobacter pylori in medium supplemented with calprotectin has shown to induce Lipid A modification, change in surface hydrophobicity as well as enhancing biofilm formation (Gaddy et al., 2015).

Changes in the charge of LPS can also explain the capsule shedding observed on isolate 391. Work done by Fresno et al. has demonstrated that the capsule is attached to LPS by ionic interactions with negatively charged residues in the core of the LPS. A change in the arrangement of the ions or a change in the charge of LPS from negative towards neutral or positive, may result in shedding of the capsule, as observed in this study, because of loss of negative charged residues necessary for capsule attachment (Fresno et al., 2006).

5 Conclusion

This study has demonstrated the use of state-of-the-art tandem mass spectrometry for tracking the interaction between the soluble components of the immune system present in serum, including the complement system. By N-terminal acetylation of peptides, it was possible to track the cleavage rates of C3, which for the serum resistant isolate 391 showed to be rapidly degraded from C3b to iC3b within the capsule. All components of the MAC was identified on isolate 391, together with the MAC inhibitor, clusterin. However, the involvement of clusterin could not explain the serum resistance, because of its deposition in the outer parts of the capsule, and thus far away from the active site on the outer membrane. This study did not reveal any novel insights in the proteolytic regulation of the complement system, that could account for the serum resistance observed for isolate 391. However, with the findings of calprotectin on isolate 391 and properdin, plasminogen and factor V on isolate 391, evidence of a change in surface charge was compiled. The change in surface charge can explain both the complement resistance and the observed capsule shedding, however further investigation must be done, to confirm this.

6 References

Albertí, S., Marqués, G., Hernández-Allés, S., Rubires, X., Tomás, J. M., Vivanco, F., & Benedí, V. J. (1996). Interaction between complement subcomponent C1q and the Klebsiella pneumoniae porin OmpK36. *Infection and Immunity*, *64*(11), 4719–4725.

Alcorlo, M., Martínez-Barricarte, R., Fernández, F. J., Rodríguez-Gallego, C., Round, A., Vega, M. C., … Llorca, O. (2011). Unique structure of iC3b resolved at a resolution of 24 Å by 3D-electron microscopy. *Proceedings of the National Academy of Sciences*, *108*(32), 13236–13240. https://doi.org/10.1073/pnas.1106746108

Álvarez, D., Merino, S., Tomas, J. M., Benedi, V. J., & Alberti, S. (2000). Capsular Polysaccharide Is a Major Complement Resistance Factor in Lipopolysaccharide O Side Chain-Deficient Klebsiella pneumoniae Clinical Isolates. *Infection and Immunity*, *68*(2), 953–955. https://doi.org/10.1128/iai.68.2.953-955.2000

Birkelund, S., Morgan-Fisher, M., Timmerman, E., Gevaert, K., Shaw, A. C., & Christiansen, G. (2009). Analysis of proteins in Chlamydia trachomatis L2 outer membrane complex, COMC. *FEMS Immunology and Medical Microbiology*, *55*(2), 187–195. https://doi.org/10.1111/j.1574-695X.2009.00522.x

Cox, J., Hein, M. Y., Luber, C. A., Paron, I., Nagaraj, N., & Mann, M. (2014). Accurate proteome-wide label-free quantification by delayed normalization and maximal peptide ratio extraction, termed MaxLFQ. *Molecular & Cellular Proteomics : MCP*, *13*(9), 2513–2526. https://doi.org/10.1074/mcp.M113.031591

Cunnion, K. M., Hair, P. S., & Buescher, E. S. (2004). Cleavage of Complement C3b to iC3b on the Surface of Staphylococcus aureus Is Mediated by Serum Complement Factor I. *Infection and Immunity*, *72*(5), 2858–2863. https://doi.org/10.1128/IAI.72.5.2858-2863.2004

Davis III, A. E., Lu, F., & Mejia, P. (2010). C1 inhibitor, a multi-functional serine protease inhibitor, 886–893. https://doi.org/10.1160/TH10-01-0073

DeLeo, F. R., Kobayashi, S. D., Porter, A. R., Freedman, B., Dorward, D. W., Chen, L., & Kreiswirth, B. N. (2017). Survival of Carbapenem-Resistant Klebsiella pneumoniae Sequence Type 258 in Human Blood. *Antimicrobial Agents and Chemotherapy*, *61*(4), 1–11. https://doi.org/10.1128/aac.02533-16

Fearon, D. T., & Austen, K. F. (1975). Properdin: Binding to C3b and stabilization of the C3b-dependent C3 convertase, *142*.

Ferreira, V. P., Cortes, C., & Pangburn, M. K. (2010). Native Polymeric Forms of Properdin Selectively Bind to Targets and Promote Activation of the Alternative Pathway of Complement. *Immunobiology*, *215*(11), 932–940. https://doi.org/10.1038/mp.2011.182.doi

Fresno, S., Jiménez, N., Izquierdo, L., Merino, S., Corsaro, M. M., Castro, C. De, … Toma, J. M. (2006). The ionic interaction of Klebsiella pneumoniae K2 capsule and core lipopolysaccharide, (152), 1807–1818. https://doi.org/10.1099/mic.0.28611-0

Gaddy, J. A., Radin, J. N., Cullen, T. W., Chazin, W. J., Skaar, E. P., Trent, M. S., & Algood, H. M. S. (2015). Helicobacter pylori Resists the Antimicrobial Activity of Calprotectin via Lipid A Modification and Associated Biofilm Formation. *MBio*, *6*(6), 1–14. https://doi.org/10.1128/mbio.01349-15

Gros, P., Milder, F. J., & Janssen, B. J. C. (2008). Complement driven by conformational changes, *8*(january).

https://doi.org/10.1038/nri2231

Hadders, M. A., Bubeck, D., Roversi, P., Hakobyan, S., Morgan, B. P., Pangburn, M. K., … Lea, S. M. (2012). Assembly and Regulation of the Membrane Attack Complex Based on Structures of C5b6 and sC5b9, *1*(3), 200–207. https://doi.org/10.1016/j.celrep.2012.02.003.LICENSING

Hallström, T., Uhde, M., Singh, B., Skerka, C., Riesbeck, K., & Zipfel, P. F. (2015). Pseudomonas aeruginosa uses Dihydrolipoamide dehydrogenase (Lpd) to bind to the human terminal pathway regulators vitronectin and clusterin to inhibit terminal pathway complement attack. *PLoS ONE*, *10*(9), 1–21. https://doi.org/10.1371/journal.pone.0137630

Harboe, M., & Mollnes, T. E. (2008). The alternative complement pathway revisited, *12*(4), 1074–1084. https://doi.org/10.1111/j.1582-4934.2008.00350.x

Holt, G. D., Pangburn, M. K., & Ginsburg, V. (1990). Properdin binds to sulfatide [Gal(3-SO4)??1-1Cer] and has a sequence homology with other proteins that bind sulfated glycoconjugates. *Journal of Biological Chemistry*, *265*(5), 2852–2855.

Jensen, T. S., Opstrup, K. V., Christiansen, G., Rasmussen, P. V., Thomsen, M. E., Justesen, D. L., … Birkelund, S. (n.d.). Complement mediated Klebsiella pneumoniae capsule changes. *Microbes and Infection*, *Submitted*.

Kidd, T. J., Mills, G., Sá-Pessoa, J., Dumigan, A., Frank, C. G., Insua, J. L., … Bengoechea, J. A. (2017). A Klebsiella pneumoniae antibiotic resistance mechanism that subdues host defences and promotes virulence. *EMBO Molecular Medicine*, *9*(4), 430–447. https://doi.org/10.15252/emmm.201607336

Kimura, Y., Miwa, T., Zhou, L., & Song, W. (2008). Activator-specific requirement of properdin in the initiation and. *Immunobiology*, *111*(2), 732–741. https://doi.org/10.1182/blood-2007-05-089821

Llobet, E., Martínez-Moliner, V., Moranta, D., Dahlström, K. M., Regueiro, V., Tomás, A., … Bengoechea, J. A. (2015). Deciphering tissue-induced Klebsiella pneumoniae lipid A structure . *Proceedings of the National Academy of Sciences*, *112*(46), E6369–E6378. https://doi.org/10.1073/pnas.1508820112

Loraine, J., Voravuthikunchai, S. P., Thomson, N. R., Taylor, P. W., Milevskyy, O., De Sousa Almeida, J., … Srimanote, P. (2018). Complement Susceptibility in Relation to Genome Sequence of Recent Klebsiella pneumoniae Isolates from Thai Hospitals. *MSphere*, *3*(6), 1–15. https://doi.org/10.1128/msphere.00537-18

Merino, S., Camprubí, S., Albertí, S., Benedí, V. J., & Tomas, J. M. (1992). Mechanisms of Klebsiella pneumoniae resistance to complement-mediated killing. *Infect Immun.*, *60*(6), 2529–2535.

Merle, N. S., Church, S. E., Fremeaux-Bacchi, V., & Roumenina, L. T. (2015). Complement system part I - molecular mechanisms of activation and regulation. *Frontiers in Immunology*. https://doi.org/10.3389/fimmu.2015.00262

Nakashige, T. G., Zhang, B., Krebs, C., & Nolan, E. M. (2016). Human Calprotectin Is an Iron-Sequestering Host-Defense Protein, *118*(24), 6072–6078. https://doi.org/10.1002/cncr.27633.Percutaneous

Pangburn, M. K., Schreiber, R. D., & Muller-Eberhard, H. J. (1981). Formation of the initial C3 convertase of the alternative pathway. Acquisition of C3b-like Activities by Spontaneous Hydrolysis of the Putative Thioester in Native C3' Be, *154*(September), 856–867.

Pragasam, A. K., Shankar, C., Veeraraghavan, B., & Biswas, I. (2017). Molecular Mechanisms of Colistin Resistance in Klebsiella pneumoniae Causing Bacteremia from India — A First Report, *7*(January).

https://doi.org/10.3389/fmicb.2016.02135

Ricklin, D., Hajishengallis, G., Yang, K., & Lambris, J. D. (2010). Ricklin D, Hajishengallis G, Yang K, Lambris JD, Complement: a key system for immune surveillance and homeostasis. *Nat. Immunol*, *11*(9), 785–797. https://doi.org/10.1038/ni.1923.Complement

Roumenina, L. T., Popov, K. T., Bureeva, S. V., Kojouharova, M., Gadjeva, M., Rabheru, S., … Kishore, U. (2008). Interaction of the globular domain of human C1q with Salmonella typhimurium lipopolysaccharide. *Biochimica et Biophysica Acta - Proteins and Proteomics*, *1784*(9), 1271–1276. https://doi.org/10.1016/j.bbapap.2008.04.029

Saggu, G., Cortes, C., Emch, H. N., Ramirez, G., Worth, R. G., & Ferreira, V. P. (2013). Identification of a novel mode of complement activation on stimulated platelets mediated by properdin and C3(H2O). *The Journal of Immunology*, *190*(12), 974–981. https://doi.org/10.1038/mp.2011.182.doi

Straus, D. C. (1987). Production of an extracellular toxic complex by various strains of Klebsiella pneumoniae. *Infection and Immunity*, *55*(1), 44–48.

Vinogradov, E., Frirdich, E., MacLean, L. L., Perry, M. B., Petersen, B. O., Duus, J., & Whitfield, C. (2002). Structures of lipopolysaccharides from Klebsiella pneumoniae: Elucidation of the structure of the linkage region between core and polysaccharide O chain and identification of the residues at the non-reducing termini of the O chains. *Journal of Biological Chemistry*, *277*(28), 25070–25081. https://doi.org/10.1074/jbc.M202683200

WHO. (2017). Global priority list of antibiotic-resistant bacteria to guide research, discovery, and development of new antibiotics. Retrieved from https://www.who.int/medicines/publications/global-priority-list-antibiotic-resistant-bacteria/en/

Xu, L., Sun, X., & Ma, X. (2017). Systematic review and meta-analysis of mortality of patients infected with carbapenem-resistant Klebsiella pneumoniae. *Annals of Clinical Microbiology and Antimicrobials*, *16*(1), 1–12. https://doi.org/10.1186/s12941-017-0191-3

Yorulmaz, S., Tabaei, S. R., Kim, M., Seo, J., Hunziker, W., Szebeni, J., & Cho, N.-J. (2015). Membrane attack complex formation on a supported lipid bilayer: initial steps towards a CARPA predictor nanodevice. *European Journal of Nanomedicine*, *7*(3). https://doi.org/10.1515/ejnm-2015-0016

Yu, Z., Qin, W., Lin, J., Fang, S., & Qiu, J. (2015). Antibacterial Mechanisms of Polymyxin and Bacterial Resistance, *2015*.